BALLISTIC FLASH CHARACTERIZATION:

PENETRATION AND BACK-FACE FLASH

THESIS

Michael J. Koslow, Second Lieutenant, USAF

AFIT-OR-MS-ENS-12-17

DEPARTMENT OF THE AIR FORCE
AIR UNIVERSITY

AIR FORCE INSTITUTE OF TECHNOLOGY

Wright-Patterson Air Force Base, Ohio

BALLISTIC FLASH CHARACTERIZATION:
PENETRATION AND BACK-FACE FLASH

THESIS

Presented to the Faculty

Department of Operational Sciences

Graduate School of Engineering and Management

Air Force Institute of Technology

Air University

Air Education and Training Command

In Partial Fulfillment of the Requirements for the

Degree of Master of Science in Operations Research

Michael J. Koslow, BS

Second Lieutenant, USAF

March 2012

AFIT-OR-MS-ENS-12-17

BALLISTIC FLASH CHARACTERIZATION:
PENETRATION AND BACK-FACE FLASH

Michael J. Koslow, BS
Second Lieutenant, USAF

Approved:

_____//signed//_____   ___28 Feb 2012__
Dr. Raymond R. Hill (Advisor)   date

_____//signed//_____   ___28 Feb 2012__
Darryl K. Ahner, LTC, USA, PhD (Reader)   date

_____//signed//_____   ___28 Feb 2012__
Mr. Jaime J. Bestard (Reader)   date

AFIT-OR-MS-ENS-12-17

Abstract

The Air Force is extremely concerned with the safety of its people, especially those who are flying aircraft. Onboard fires caused by munitions fire present a very real and dangerous threat. In order to help negate these incidents, analysts must be able to predict the flash that can occur when a projectile strikes a target. This thesis extends past AFIT research in developing a model to characterize a back-face flash, given a fragment penetration and a back-face flash occurs.

The methodology in this research directly continues AFIT work for the 46th Test Group, Survivability Analysis Flight. It examines models to predict penetration of a fragment fired at a target and provides a first glance at an empirically-based likelihood of a penetration. Empirical live-fire fragment test data are used to create an empirical model of a flash event. The data are used to conduct statistical validation efforts. The resulting model provides an initial back-face flash modeling capability and was delivered for implementation in joint survivability analysis models.

To My Fiancée

Acknowledgements

Table of Contents

List of Figures

List of Tables

BALLISTIC FLASH CHARACTERIZATION:
PENETRATION AND BACK-FACE FLASH

1. Introduction

1.1. Background

Aircrew members flying combat missions are concerned with the chance that a

fragment from an exploding threat device may penetrate into the airframe to possibly

ignite a fire onboard that aircraft. The term *vulnerability* refers to "the inability of the

aircraft to withstand the hit" by an air defense (Ball, 2003). One concern for

vulnerability revolves around a *flash* that may occur when a projectile strikes and

possibly penetrates an aircraft's fuselage. When certain fired rounds strike the airframe,

they break into fragments called *spall*. The kinetic energy from the projectile is

"dissipated in various forms, mainly through plastic deformation of the target, friction,

and heat" (Bestard & Kocher, 2010). Spall and other fragmentation from an impact often

times gain enough thermal energy to oxidize the materials involved (Bestard & Kocher,

2010). This oxidation causes a *flash*.

The danger with any flash associated with the airframe is that the flash can ignite

a fire which may come in contact with fuel, possibly causing an explosion. In order to

prevent such a travesty from occurring, analysts must be able to characterize such flashes

so effective countermeasures can be devised, examined, and employed. The ability to

characterize the flash permits analysts to study the flash's effects and the utility of

possible countermeasures within an analytical framework. The 46th Test Group,

Survivability Analysis Flight has worked for several years on developing a way to

characterize these flashes based on various projectile inputs, such as velocity, obliquity,

material type, and material thickness. Over the years, numerous people have tackled parts of the problem.

A designed experiment of high velocity fragments shot into various materials representing aircrafts resulted in a database of high-speed video of flash events. These flash videos were then processed from still frame images into data characterizing the flashes using ellipses enclosing the flashes, over the time duration of the flash. This processing provided a time series of data describing the size and position of flashes both on the impact (entry) side as well as on the exit (back) side. A model was designed to predict the size of the flash across time based on various inputs (Henninger, 2010). This model was then revised to better fit the data generated from the flash video data processing (Talafuse, 2011).

1.2. Problem Statement

Talafuse (2011) gave an initial entry side flash model. Peyton (2012) extended and refined the initial model, which only focused on the entry side flash. This work adds another piece towards the final objective of producing an overall flash model by adding the exit side, or back-face, flash which can help to predict the critical flashes which cause onboard fires. Specifically, this work examines the probability of penetration and a back-face flash, and assuming a back-face flash occurs it extends the current research to provide a model to characterize such a flash. This work represents an initial back-face flash model; a model of the flash inside the airframe body given fragment penetration of the airframe skin.

The 46th Test Group, Survivability Analysis Flight has sponsored the research throughout, and various employees and students have contributed to the effort. Bestard

and Kocher (2010) developed the methodology to capture flashes with high-speed video. Henninger (2010) established the ability to use regression-based techniques in order to model the radius of a flash. Talafuse (2011) continued that work and developed an initial methodology to convert the data into a usable predictable model. Peyton (2012) further improved the model to make it more accurate and modeled the front-face flash. This work takes a look at current methods to predict a penetration of a materiel, gives an initial look at probability of a back-face flash given input parameters, provides the model for the back-face flash assuming one occurs, employs cross-validation techniques to verify the validity of the models, and paves the way for the final stage in the continued work: to transition the model to the analysis community and to validate the models with live-fire tests.

1.3. Thesis Layout

Chapter 2 provides a review of pertinent past research in this area along with background information concerning the data. Chapter 3 provides a look at the penetration aspect of the research, namely whether certain input parameters result in a penetration as well as a first-look model as to whether the certain input parameters result in a back-face flash. Chapter 4 develops models to characterize the back-face flashes, given they occur, and provides validation of these models. Chapter 5 provides a conclusion.

2. Literature Review

This chapter reviews the previous work that has paved the way for the current research. While it does not give full details of past research, it gives a general understanding. This chapter also provides an understanding of the techniques and processes used in the research.

2.1. Flash Characterization Effects

Past research dates back to the early 1990s with four AFIT Master of Science theses. Reynolds (1991) focused his research on incendiary functioning (IF) of armor-piercing incendiary (API) projectiles impacting graphite and epoxy composite panels, as opposed to metal targets as had been used most often in the past. He based his analysis on four predictor variables: impact velocity, impact mass, ply thickness, and impact obliquity angle. He developed two regression models: the first classified front-face functioning as actual functioning that could ignite fuel, while the second classified it as a non-function.

Knight (1992) expanded Reynold's work continuing with the API projectile function. Using regression analysis, discriminant analysis, and neural networks, he better predicted residual velocity, residual mass, and incendiary functioning for API rounds on graphite/epoxy composite panels. He determined that a neural network algorithm with three categories (frontal, mixed functioning, and nonfunctions) worked the best.

Lanning (1993) studied the effects of penetration of two composite panels and found that composite panels require a higher projectile velocity to produce flashes than aluminum panels. He also discovered that these flashes lasted longer in duration. This discovery led Blythe (1993) to establish a methodology for predicting flash

characterization of projectile impacts with composite materials. Blythe noted that back-face flashes had not received much attention.

2.2. Reducing Flash Events into Time Series Data

Bestard and Kocher (2010) formulated the first piece of the current research thread. They understood that the survivability community needed a standardized data collection methodology with corresponding valid and verified models. With the advance of impacting technology, the ballistic impact flash can be recorded on high-speed digital video. This video can be examined frame-by-frame, so they were able to use it to examine and analyze the flash size and position at each frame. Using a least squares minimization technique, they analyzed the flash in each frame and enclosed the flash in an ellipse, with the ellipse size a function of the user-defined flash intensity level. They quantitatively described various characteristics of the flash, including the ellipse positions, sizes, and orientations as a function of time. This led them to determine that the flashes follow the projectile's trajectory with a logarithmic behavior. They also determined that the size and shape of the cloud generally follows a Weibull function over time.

By capturing this data, they paved the way for future development of a predictive flash model. They expressed the desire that a final model be developed to predict flash position, size, orientation, and thermal energy released as a function of time, based upon projectile and target properties and impact conditions.

2.3. Initial Flash Event Model

Henninger built a time-based empirical function to model the flash-event time-series data. He used data from an experiment that used projectile weight, projectile velocity, target panel thickness, and impact obliquity as its factors. However, his final model only predicted the flash radius as a function of time instead of as functions of the input parameters since he was modeling specific flash events. He also studied just the front-face flash, not the back-face flash. His initial theory was that he could model the flash radius as a regression-based model with normally-distributed error. His base model took the form:

$$FlashRadius = F(time) + N(0, \sigma^2) \tag{1}$$

His analysis led him to apply a quartic model to fit the flash radius for both the X and Y radius. His models took the form:

$$r_{xi}(t) = \beta_{x1}t + \beta_{x2}t^2 + \beta_{x3}t^3 + \beta_{x4}t^4 + \epsilon_{xi} \tag{2}$$

$$r_{yi}(t) = \beta_{y1}t + \beta_{y2}t^2 + \beta_{y3}t^3 + \beta_{y4}t^4 + \epsilon_{yi} \tag{3}$$

After studying his results, he deemed that the error was not simply normally-distributed but instead was also time based and autocorrelated. However, his initial model laid a foundation for subsequent meta-model development.

2.4. Initial Meta-Model of Flash Events

Talafuse (2011) built upon Henninger's work, primarily by creating a meta-model that would provide a predictive model over time for a flash based on the projectile conditions that Henninger had used as input factors. Talafuse also found limitations in the previous test data which Henninger (2010) and Bestard and Kocher (2010) both used.

The recorded shots were biased because several flashes from the shots were not entirely

caught on camera (they moved out of the frame of view) and thus did not represent the

entire spectrum of possible data points. In other words, results from a full factorial test

were not present. While he still had to use the data available to him, he helped design a

full factorial model which was run after completion of his thesis research. The results

from that future test were then used by Peyton (2012) as well as in this thesis.

While validating the data that he did have, Talafuse discovered that some shots

were unusable. He was able to correct several sign reversal issues as well as identify that

user inputs regarding flash intensity caused biased radii measures. These efforts refined

the video processing methods used to create the flash event time series data. Talafuse

expanded Henninger's analysis by using the input factors to produce coefficients for each

factor. He ran models for each flash event, recorded the model coefficients, and then

sought a meta-model of the design parameters with which to predict the flash event

model. As opposed to just having a model based on time, the quartic model coefficients

were themselves determined using a regression equation. In the meta-model, each

coefficient is predicted using an equation of the form:

$$\beta_i = b_0 + b_1 Thick + b_2 Angle + b_3 Mass + b_4 Vel, i = 1,..,4 \qquad (4)$$

After analyzing the results, Talafuse concluded that, contrary to Henninger's

findings, flash radius could not be predicted with sufficient fidelity when using all four

design factors because such a model was overspecified. To correct for this error, he

developed models after grouping shots by panel thickness, which provided more accurate

results. Initial looks led him to conclude that the flash orientation angle had no visible

patterns, however further analysis revealed that the orientation seemed to be centered

around a zero radian angle and follow a normal distribution. He also determined that the flash orientation was not time dependent but rather modeled as a random draw and held constant for the duration of the flash. The center position of the flash was time-dependent, although it had no correlation with the test scenario parameters. Talafuse's (2011) final result was an initial model for predicting the boundary of a ballistic impact flash event.

2.5. An Improved Flash Model Approach

With the results of the designed experiment developed by Talafuse (2011), Peyton (2012) had new data to analyze. Instead of the original 21 usable data points, Peyton now had 283 suitable shots with which to analyze the front-face flash. After some analysis, Peyton determined that the Weibull function was a better fit of the data than was the quartic function used by Talafuse (2011). He ran regressions which generated numbers to create the model coefficients. These generated numbers are the *b*'s in this calculation:

$$Model\ Coefficient = e^{(b_0 + b_1(vel) + b_2(oblq) + b_3(thick) + b_4(mass))} \tag{5}$$

where *vel* is the measured velocity of the shot, *oblq* is the angle of obliquity between the target plate and the show axis, *thick* is the thickness of the target plate, and *mass* is the mass of the fired projectile. The resulting model coefficients were the gammas and betas for the meta-model. His baseline meta-model took the form:

$$FlashRadius_x(t) = \gamma_x\left(\left(\frac{\alpha}{\beta_x}\right)\left(\frac{t}{\beta_x}\right)^{(\alpha-1)} e^{-\left(\frac{t}{\beta_x}\right)^{\alpha}}\right) \tag{6}$$

$$FlashRadius_z(t) = \gamma_z\left(\left(\frac{\alpha}{\beta_z}\right)\left(\frac{t}{\beta_z}\right)^{(\alpha-1)} e^{-\left(\frac{t}{\beta_z}\right)^{\alpha}}\right) \tag{7}$$

The meta-model generates the radius of the flash over time. This model is the meta-model Peyton provided for the front-face flash.

Peyton also performed other analysis on the front-face flash. He determined that there was not a definitive relationship between shot parameters and the flash position. The data set used by Peyton was partitioned into two sets, A and B, which were used for cross-validation purposes. Models built using set A were used to predict set B data, and vice versa. After successful cross-validation, the entire data set was used to build the final front-face model. Equations 5-7 were adapted for the back-face flash models developed in this research and the same data partitioning was used for cross validation purposes.

2.6. The Data

The data used for this portion of the research was gathered by the 46th Test Group, Survivability Analysis Flight. They ran an experiment that Talafuse (2011) helped design. In this experiment, they were concerned with five main factors. Those factors, and their levels, are shown in Table 1 below. Note two material types are used; meta-models are built for each material type.

Factor	Variable	Low	Mid1	Mid2	High	Units
Initial Velocity	Vel	4000	N/A	N/A	7000	fps
Obliquity Angle	Angle	0	N/A	N/A	45	degrees
Material Type	Mat	2024	N/A	N/A	7075	N/A
Panel Thickness	Thick	0.063	N/A	N/A	0.25	inches
Penetrator Size	Mass	20	40	75	150	grain

Table 1: Designed Experiment Factors and Levels

A full-factorial design means that every possible combination of factor levels is run; an experimental data point is present regardless of which combination of the five factors you choose. A replication means that a given combination of factors at specified levels is taken more than once. For this experiment, there are four factors with two levels and one factor with four levels. A full factorial design for this experiment involves 2^4*4^1, or 64 design points. Replicating this design 5 times means that the final design has 320 shots. The parameters for each shot can be found in Appendix A. To prevent bias and to help calibrate the machinery and cameras, 30 additional shots were added as initialization data but are not included in the analyzed results. Altogether, the designed experiment required 350 shots.

High-speed digital cameras captured each shot from both a top view (Z-axis) and a side view (X-axis). The footage was then digitally processed and the parameters for each shot were recorded in its own excel spreadsheet. Each spreadsheet also contained measurements of each resulting flash. For various time steps, parameters for an ellipse which enclosed the flash were recorded. These parameters included center position of the ellipse, radius in each direction, rotation angle, area, and distance of the center of the flash from the origin.

One issue with the data was that time recorded for each shot was on a small scale (measured in milliseconds). If a regression containing the raw time files was performed then the coefficient for the time step would be extremely large compared to the other factors, and the computational round-off error could greatly affect the results. To correct for this problem, the raw time was converted into a scaled time. The raw time was

divided by 0.000121 seconds, providing a scaled time for each time step. This alleviated round-off error issues due to scaling.

Another issue with the data was that not all 350 shots could be used. Seventeen of the shots were in error, leaving 333 shots. Of these, 25 were removed because they were calibration runs, leaving 308 shots to be analyzed. In order to be usable data for function fitting, there needed to be at least three recorded data points. This criterion eliminated 53 of the shots, leaving 255 points. At this point, each shot video was viewed to determine whether or not a back-flash occurred. Of the 255 remaining shots, 199 of them had adequate back-face flashes.

Two different materials were used in this data set: 7075 aluminum and 2024 aluminum. Meta-models are created for each material type. The 199 usable back-flash shots were separated by material type into two sets of data: 98 shots for the 7075 aluminum and 101 for the 2024 aluminum. The data for these shots can be found in the accompanying spreadsheet under the tab "Back-Face Flash Data".

2.7. Penetration Equations Handbook for Kinetic-Energy Penetrators

In the 1970s, vulnerability assessments with respect to aircraft penetration were "being made on a large scale with different organizations either working on separate portions of a single analysis or on interrelated analyses." (JTCG/ME, 1985, p. 1) Since various organizations relied on the same general analysis, consistent analytical procedures were needed to ensure that each organization could make meaningful comparisons with each other. To accomplish this task, the vulnerability community formed the Penetration Equations Committee of the Joint Technical Coordinating Group for Munitions Effectiveness (JTCG/ME). In 1977, they produced The Penetration

11

Equations Handbook for Kinetic-Energy Penetrators. This handbook provides

procedures and penetration equations based on a review of available data and theories at

the time for terminal ballistics of projectiles and fragments impacting aircraft targets.

Over the years, it has been updated to accommodate new procedures. While the

handbook provides the most detailed procedures, a brief overview is provided.

The Figure 1 schematic outlines the iterative process used for representing

projectiles, showing the interrelation of the stages and the principal computations.
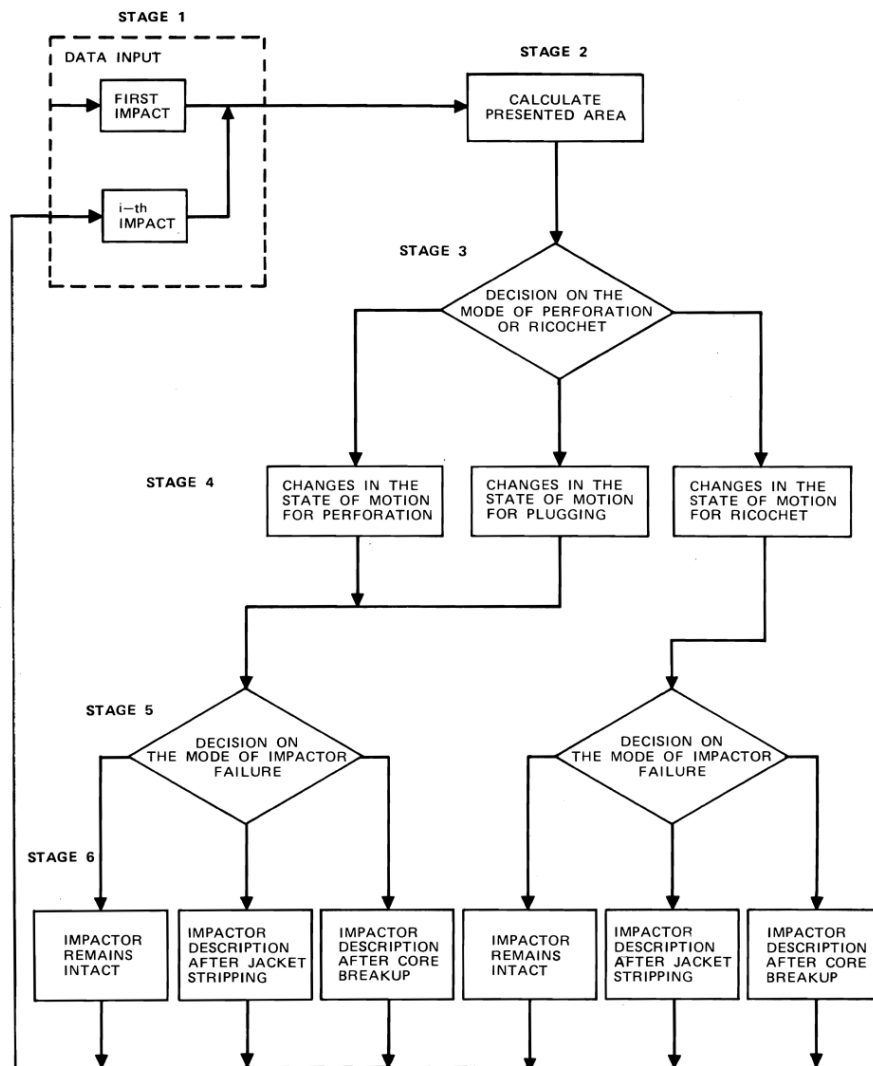
Figure 1: A Schematic Representation of the Principal Computations for Projectiles
(JTCG/ME, 1985, p. 11)

The six stages correspond to six equations, parts of two sets. The first set "predict the state of the impactor for certain ranges of impact conditions", and the second set "determine the range of impact conditions for which specific equations of the first type apply." (JTCG/ME, 1985, p. 11) The six parts are as follows:

1. Input of impactor and target data;
2. Determination of impactor presented area and shape;
3. Determination of the mode of perforation or ricochet;
4. Calculation of impactor changes of motion;
5. Determination of impactor mode of failure; and
6. Calculation of changes in the description of the impactor.

The input data covers factors of both the projectile and the target. These factors include Material Properties (elastic modulus, specific weight, density, tensile strength, brinnel hardness), Principal Dimensions (length, nose length, thickness, diameter, nose angle, weight), Functional Capacity (incendiary), and State of Motion (projectile speed, aircraft speed, speed in component frame of reference, yaw, obliquity, azimuth angle of shotline, elevation angle of shotline). Basically, equations are executed at each stage. The result directs the way through the schematic, where further calculations are performed. At the end of stage 6, the resulting parameters are returned to stage 1 as new input parameters.

The previous schematic shows the process specifically for full rounds. For experiments like the one used in this research, which uses fragments as opposed to full rounds, several changes occur. They are: (1) the "input data, (2) the use of a single blunt perforation process for all fragments, and (3) the recognition of different failure modes for steel fragments." (JTCG/ME, 1985, p. 33) Figure 2 is the schematic for fragments:
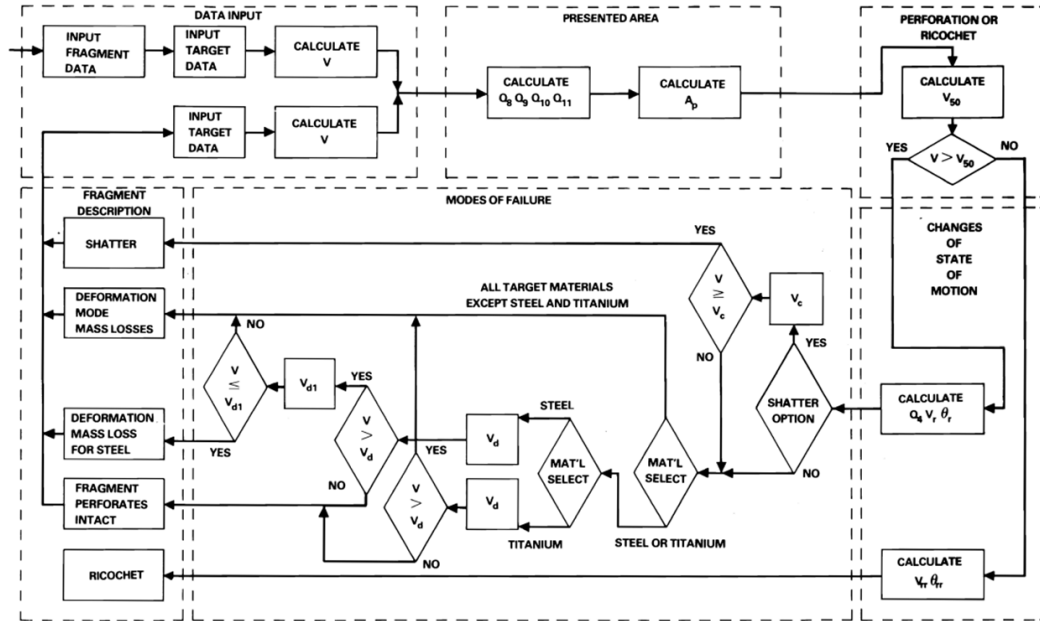
Figure 2: A Schematic Representation of the Principal Computations for Fragments
(JTCG/ME, 1985, p. 34)

The input data is reduced to factors of the Material Properties and State of

Motion. Notice this doesn't have the Principal Dimensions or Functional Capacity that

the equations for the full rounds had. Through all of the calculations, the one this thesis

is most concerned with is the result of the Fragment Description section. The four

possible results from this stage are "(1) perforation of the fragment intact, (2) a

deformation mode of mass loss, (3) a special deformation-mass loss calculation for steel

targets, and (4) shattering of the fragment." (JTCG/ME, 1985, p. 40)

Upon examination of the handbook, the abundant equations and various paths can

seem overwhelming. They are not easily interoperated or easy to follow. In order to

facilitate these calculations, the Applied Research Associates, Inc. (ARA) developed the

Fast **A**ir **T**arget **E**ncounter **PEN**etration Program (FATEPEN). This program was

developed for the Naval Surface Warfare Center, Dahlgren Division (NSWC/DD). The

program represents the current model used to predict penetration for fragments. Its logic

is discussed in the next chapter.

3.   Penetration Aspect

This chapter looks into first of two major portions of the research: whether or not a projectile will penetrate the material it strikes, and whether or not the penetration results in a back-face flash. The areas addressed include the application of the current model, the validation of this model, and a first look at the probability of a back-face flash given that a penetration occurs.

3.1. Current Model

The current model for predicting penetration is based on the Fast Air Target Encounter Penetration (FATEPEN) Program developed by Applied Research Associates, Inc. (ARA). "FATEPEN is a set of fast running algorithms which simulate the penetration of and damage to spaced target structures." It was developed using both fundamental principles of mechanics as well as from experimental procedures. The model is updated over time with new versions as more information becomes available. While FATEPEN has several functions, the aspect of FATEPEN used for this research regards its simulation of the penetration. In particular, it's concerned with the probability of a penetration given certain input parameters. "The penetration algorithms are comprised of deterministic, analytical/empirical engineering models." (SURVIAC)

Mr. Timothy Staley, a vulnerability analyst from the Aeronautical Systems Center Engineering Directorate, Combat Effectiveness and Vulnerability Analysis Branch (ASC/ENDA), provided expertise in the execution and application of FATEPEN. FATEPEN does not provide a percentage probability of penetration in the way that would have directly correlated to the test data. Instead, the program produces a *V50* value given a set of inputs for the penetrator and the target. This value is the velocity, in feet per

second, which has been experimentally determined to provide a 50% chance of penetration. In other words, given the input parameters, if you fire the projectile at the V50 velocity then half of the time you will see a penetration and the other half of the time you will not. The benefit to knowing this value is that a relative probability can be drawn from that information. If the V50 value is 1000 fps and you fire a shot at 100 fps, the probability of a penetration is extremely low; similarly, if a projectile is shot at 5000 fps, a penetration is almost guaranteed. More detailed assessments of predicting penetration based upon input parameters are currently unavailable.

In an attempt to further validate the V50 value, the experimental parameters for the shot were inserted into FATEPEN. The results can be seen in Table 2 on the next page.

Obliquity	Material	Thickness	Frag Size	V50
0	2024	0.063	20	620.57
0	2024	0.25	20	1557.08
0	7075	0.063	20	606.23
0	7075	0.25	20	1649.55
45	2024	0.063	20	792.53
45	2024	0.25	20	2108.55
45	7075	0.063	20	774.22
45	7075	0.25	20	2233.76
0	2024	0.063	40	584.99
0	2024	0.25	40	1160.15
0	7075	0.063	40	566.59
0	7075	0.25	40	1207.35
45	2024	0.063	40	743.23
45	2024	0.25	40	1548.99
45	7075	0.063	40	719.85
45	7075	0.25	40	1612.01
0	2024	0.063	75	564.76
0	2024	0.25	75	934.40
0	7075	0.063	75	544.05
0	7075	0.25	75	955.85
45	2024	0.063	75	714.71
45	2024	0.25	75	1233.95
45	7075	0.063	75	688.51
45	7075	0.25	75	1262.27
0	2024	0.063	150	552.18
0	2024	0.25	150	794.12
0	7075	0.063	150	530.04
0	7075	0.25	150	799.57
45	2024	0.063	150	696.31
45	2024	0.25	150	1037.82
45	7075	0.063	150	668.39
45	7075	0.25	150	1044.95

Table 2: V50 values

The thickness seemed to have the largest effect on the V50 value. Shots with a thickness

of 0.063 inches ranged from 530 fps to 793 fps, with an average of 648; shots with a

thickness of 0.25 inches ranged from 794 fps to 2234 fps, with an average of 1321 fps.

Since the experiment tested target velocities at 4000 and 7000 fps, which are far above

the average values, every experimental shot should have resulted in a penetration. After examining the original views of each shot, this fact was validated.

3.2. Characterization Percentages

FATEPEN provided a value for judgment as to whether or not a penetration occurred. However, a penetration does not correlate to a back-face flash. No current model exists to predict the likelihood of a back-face flash given that a penetration has occurred. While the current data is fairly limited, it can still be used to provide a baseline upon which further analysis can be completed by providing the percentage of the times flashes occurred with each setting.

In order to present these percentages, the present data had to be analyzed. After compiling each shot into one master list with its parameters, the shots were separated into whether or not a back-flash occurred. Of the 255 usable data points, 199 had adequate back-flashes while 56 of the shots did not. Overall, that meant that 78% of the shots fired in the design had flashes. The shots were then characterized by each level and factor and are summarized in Table 3 below:

Target Velocity	% Flash	Thickness	% Flash
4000	49.52%	0.063	83.46%
7000	98.00%	0.25	72.66%
Obliquity		Target Size	
0	84.96%	20	63.64%
45	72.54%	40	75.38%
Material		75	84.75%
2024	79.53%	150	89.23%
7075	76.56%		

Table 3: Penetration and Back-Flash Percentages by level

Table 3 provides some quick insight into the important factors with regards to a flash. Clearly, the faster the penetrator is traveling the more likely that a back-face flash occurs. Obliquity, target material type, and target thickness do not appear to have a large effect on the occurrence of a back-face flash. The larger the penetrator's size the more likely a back-face flash is to occur. While these percentages are not a model to predict the occurrence of a back-face flash, they certainly provide some insight which can be studied in more detail in the future.

Although not ideal because of the limited data, an initial model based on the input parameters was attempted. The 255 valid data points were entered into JMP with a binary variable referring to whether or not a back-flash occurred: data points with a flash received a value of *1* while those without a flash received a value of *0*. The measured velocity, obliquity angle, target thickness, and penetrator measured size were all entered as continuous variables and effects, while material type was nominal and had equations based off each material type. A simple regression was then run on the data to predict the response of the binary flash variable (modeled as a continuous variable).

Due to the narrow scope of the data points, the results were not great. Although the model JMP developed indicates that velocity and size are significant for both material types and that thickness is significant when shooting at 2024 aluminum, these results must be taken with a grain of salt. Both models display that a significant lack of fit exists. Strong evidence also exists of non-constant variance. So while the actual numbers should not be used to predict the occurrence of a back-face flash, this model does provide a basis for future studies to refine such a model. The results from this model can be found in Appendix B.

3.3. Future Studies

Contrary to original beliefs, no current model exists to predict the existence of a back-face flash given that a penetration occurs. While the percentages provided in the section above give a starting point, an actual model would be preferred. The regression run using JMP needs further analysis in order to become worthwhile, or perhaps a completely different approach could be taken. A possible extension is to consider a neural network or logistic regression approach, similar to the approaches used in the past research discussed in Chapter 2.

4. Back-face Flash Development

This chapter provides the bulk of the contribution to the current process. It provides the model to characterize a back-face flash, given that one occurs. The chapter explains the process, explains various validation techniques, provides the cross-validation results, provides the final overall model given to the client, and gives recommendations for future studies.

4.1. Process

For this analysis, data from the top-view of the flash were used because it provided more usable data points than did data from the side-view of the flash. Thus, the model predicts flash on the X-Z plane versus the X-Y plane used in Talafuse (2011). The final code used to create the back-face meta-model was developed by Peyton (2012) and adapted for a back-face flash model. In order to use that code, the data needed to be gathered into a certain format. The data representing the ellipses over all time periods resulted in 350 shots. However, 17 of the shots had error and were omitted, leaving 333 shots. Another twenty-five were removed as calibration runs. Since the Weibull model used requires at least three recorded data points, another 53 shots were eliminated. Of the remaining shots, 199 had adequate back-flashes. Of these 199 shots, 98 were from the material 7075 aluminum while 101 were from 2024 aluminum. These shots were separated leaving two large groups of data. An Excel file provided the format necessary to read the data into Matlab in order to execute that code.

4.1.1. Model Development

After converting the data from the Excel files into Matlab files, the Matlab .m

script processed each shot and provided coefficients for the meta-model. The meta-

models for each material are shown in the following tables:

	X-direction			Z-direction	
	β	γ		β	γ
velocity	2.62E-05	0.000328		-2.08E-05	0.000527
obliquity	-0.003791	0.01852		0.004288	0.005618
thickness	-0.560012	-0.7615		-0.58819	-3.36013
mass	0.0014186	0.009403		0.002938	0.010569
intercept	1.7042617	3.039882		1.593113	2.468511

Table 4: 7075 Aluminum Full Model

	X-direction			Z-direction	
	β	γ		β	γ
velocity	1.41E-04	0.000444		6.19E-05	0.000738
obliquity	-0.00435	0.014743		0.00267	0.001499
thickness	0.40562	-0.36829		0.456721	-3.2996
mass	0.001821	0.01093		0.002458	0.010505
intercept	0.775179	2.09957		0.959158	1.193209

Table 5: 2024 Aluminum Full Model

These numbers represent the meta-model coefficients used to calculate the coefficients

for the time-series models used to predict flash radius over time. These models were

transitioned to the 46th Test Group, Survivability Analysis Flight.

The general equation for the probability density function of a Weibull random

variable t, as presented in Peyton (2012), is:

$$f(t; \beta, \alpha) = \begin{cases} \gamma * \dfrac{\alpha}{\beta}\left(\dfrac{t}{\beta}\right)^{\alpha-1} e^{-(t/\beta)^t} & t \geq 0, \\ \\ 0 & t < 0 \end{cases} \tag{8}$$

Where β is the shape parameter, α is the scale parameter, and γ is a multiplier. Peyton

(2012) determined that a scale parameter of $\alpha = 1.5$ provided the best general look of what

a time-flash should look like. The derived models in the tables above each have two columns of numbers for each direction (X and Z): the first column corresponds to the shape parameter (β) for the Weibull distribution while the second column is a coefficient (γ) which is multiplied times the entire equation. In order to generate β and γ, Equation 5 is used. For a given set of input parameters, each value is multiplied with its corresponding coefficient from the generated model, such as Table 4 or Table 5. For example, Shot 210 involved 2024 aluminum and had the following parameters: vel = 3998 fps, $oblq$ = 45 degrees, $thick$ = 0.063, and $mass$ = 73.36 grains. The b coefficients in Equation 5 to calculate β in the X-direction come from Table 5, first column because it corresponds to the X direction and the shape parameter. Inserting these values into Equation 5 yields the following:

$$\beta = e^{(0.775179+0.000141*3998-0.00435*45+0.40562*0.063+0.001821*73.36)}$$

$$\beta = 3.671.$$

And from the second column, for the multiplier:

$$\gamma = e^{(2.09957+0.000444*3998+.014743*45-0.36829*0.063+0.01093*73.36)}$$

$$\gamma = 203.719.$$

With the above variables calculated, the individual model for the X direction for shot 210 can be represented as follows:

$$f(t; 3.671, 1.5) = \begin{cases} 203.719 * \left(\dfrac{1.5}{3.671}\right)\left(\dfrac{t}{3.671}\right)^{0.5} e^{-(t/3.671)^t} & t \geq 0, \\ 0 & t < 0 \end{cases}$$

$$f(t; 3.671, 1.5) = \begin{cases} 83.249 * \left(\dfrac{t}{3.671}\right)^{0.5} e^{-(t/3.671)^t} & t \geq 0, \\ 0 & t < 0 \end{cases} \tag{9}$$

For each time step, the above equation is evaluated to predict the flash at that time. The same process is repeated for both directions (X and Z), and for every shot.

The following graph shows the X-radius of the predicted flash as well as the X-radius of the actual flash:
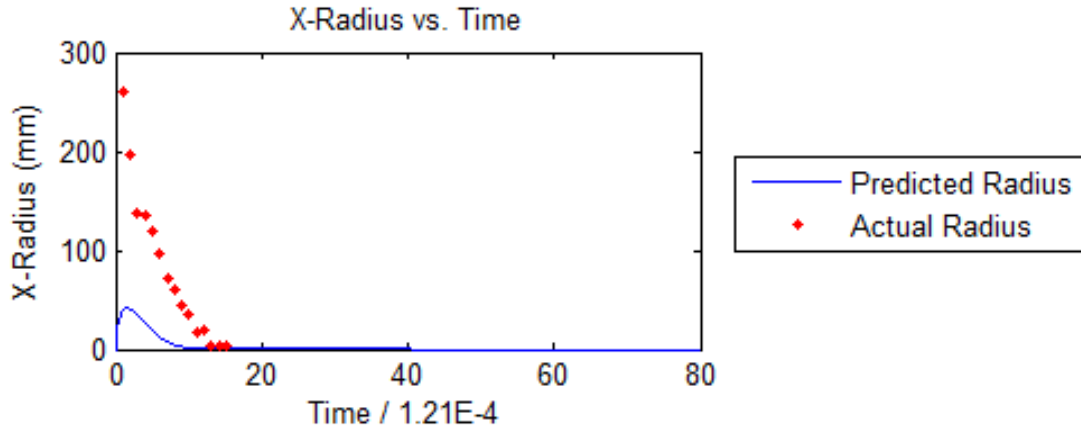
Figure 3: Shot T210 Flash X-Radius vs Time

The blue line shows Equation 9 evaluated at each time step, which is the time *t* divided by 0.00121. Based on this graph, it appears that the predicted flash was smaller than the actual flash that occurred. More discussion on the analysis of the flash comes later.

4.2. Statistical Methods

One of the most important parts of empirical model development and analysis is demonstrating that the model is valid. Because the full model was developed using all of the data points, it cannot directly be validated with that data. Clearly the points used to generate the model should closely follow the results of the model. In order to show that the model is valid, one must test the model on data that was not used to create the model. Cross-validation is a commonly used methodology.

The original data was randomly divided into two separate sets for each material type, labeled Set A and Set B. With two separate sets of data points, a model is developed using Set A and used to predict Set B. The roles of each set are then reversed. The accuracy of each prediction effort is then examined. This approach removes any

24

potential bias from a data point creating the model also being tested in it. In regression

modeling, this is referred to as double-cross validation (Montgomery, Peck, & Vining,

2006, p. 313). Clearly, if each sub-model effectively predicts the other set, then the

combined model can be expected to accurately represent the overall flash characterization

for that material. Several different statistical methods exist to demonstrate how

accurately one model predicts another set of data. This research uses several different

techniques to report the accuracy of their models: the residual mean square (commonly

denoted R^2), mean square error (MSE), and *area under the curve*.

4.2.1. Residual Mean Square

Residual Mean Square (R^2) was initially chosen as a comparative metric because

it is relatively easy to understand and was already being utilized by the Survivability

Analysis Flight. The R^2 value indicates the proportion of variability around the mean

explained by the regression in the model. In general, the scale is from 0 to 1, where 0

means that the regression in the model does not explain any variance and a value of 1

means that one-hundred percent of the variance is explained. The R^2 value is calculated

by taking the ratio of the variation in the data points explained by the regression over the

total observed variation. In other words, it is the sum of squares from regression over the

total sum of squares. The formula, as presented by Montgomery, Peck, and Vining

(2006, p. 44), is below:

$$R^2 = \frac{\sum_{i=1}^{n}(\hat{y}_i - \bar{y})^2}{\sum_{i=1}^{n}(y_i - \bar{y})^2} = \frac{SSreg}{SStot} \tag{10}$$

where n = number of data points, $\hat{y}_i$ = the ith predicted value, $\bar{y}$ = the mean of the

responses, and y_i = the measured value of the ith data point. This equation is based on

the assumption that the total sum of squares is equal to the addition of the residual sum of squares and the explained sum of squares. This equation also forces the regression line of value versus response to run through the origin.

An alternative to this model is one which does not have an intercept. The R_0^2 value is calculated by taking the ratio of the variation in the data points explained by the residuals over the total observed variation and subtracting it from one. In other words, it's the sum of squares from error over the total sum of squares subtracted from one. The formula, as presented by Montgomery, Peck, and Vining (2006, p. 45), is below:

$$R_0^2 = 1 - \frac{\sum_{i=1}^n (y_i - \hat{y}_i)^2}{\sum_{i=1}^n (y_i - \bar{y})^2} = 1 - \frac{SSerr}{SStot} \tag{11}$$

where n = number of data points, $\hat{y}$ = the predicted value, $\bar{y}$ = the mean of the responses, and y_i = the measured value of the ith data point.

Clearly an R^2 value closer to one is preferred to one close to zero because it indicates that the model is strong at predicting the response. However, increasing the R^2 value is not always beneficial. Montgomery states that "in general, R^2 never decreases when a regressor is added to the model, regardless of the value of the contribution of that variable." (Montgomery, Peck, & Vining, 2006, p. 83) In other words, adding a variable can only help explain the variance. At a certain point the additional regressors force the model to become over-specified. The model becomes too closely based on the data which were used to make it and it loses its robustness. This fact makes it difficult to have a definitive "best value" for R^2.

The biggest problem with using R^2 as the only statistical method to determine significance is that it does not always stay in the range from 0 to 1, particularly with Equation 11. When the residual sum of squares (denominator) is large, it is possible to

make the R_0^2 value negative. In these cases, the value becomes useless to an analyst. So while it can be very easy to understand because of its relative scale, another method is needed to always provide a basis for analysis.

4.2.2. Mean Square Error

An alternative way to describe the accuracy of a model involves the Mean Square Error (MSE). This term is sometimes referred to as Mean Square Residuals. The formula for calculating MSE, as presented by Montgomery, Peck, and Vining (2006, p. 267), is below:

$$MSE = \frac{\sum_{i=1}^{n}(y_i - \hat{y})^2}{n - p} = \frac{SSerr}{n - p} \tag{12}$$

where n = number of data points, $\hat{y}$ = predicted value, y_i = measured value of the ith data point, and p = number of estimators.

Unlike R^2, there is no common scale for MSE. While a lower value of MSE is desired, there is no upper limit on what the value of MSE can be. The numerator in the equation is equivalent to the error sum of squares (SS_{res}). As the number of estimators, p, increases, the SS_{res} will always decrease because more factors are present to explain the error. For a time, increasing p will decrease MSE, just like adding factors will lead to an R^2 value closer to one. However, MSE also has the denominator. At a point, the amount of decrease in SS_{res} will not compensate for the fact that the denominator is also decreasing. At this point, adding additional estimators will actually increase MSE and provide a worse result.

One concern with using MSE to evaluate model effectiveness is that MSE can vary largely depending on the regression with which it is used. Trying to compare an

27

MSE of a model with one set of data to a model with another set of data does not always accurately reflect which one is "better". On the other hand, because there is not a standard scale there is not the danger of "improving the model" by working toward a desired number.

4.2.3. Area under the curve

Another alternative to the above approaches is to take the *area under the curve*. This approach shows a graph of the radius of the flash at each time step and calculates the area that this curve covers. An advantage to such an idea is that it allows a methodical statistical approach to analysis that can easily be converted into sensible data. If one line is always above the other, then a ratio of the area that the predicted model covered against the area that the actual data covered shows how closely the model represents the real data. If the lines cross each other, then the numbers become more complicated, but a visual check can still show generally how close the model predicts the data.

In many cases, calculating the *area under the curve* requires integration. However, these data include specific time steps and are not continuous. This fact causes the "graph" to be several bars close together. The benefit to this setup is that the area can simply be calculated by taking the height of the curve (the radius), since each time step is one unit long and multiplying the radius by the time (one) is still the radius. By adding the radii at each time together, the area is derived.

Several different aspects of the area were recorded. First, separate calculations occurred for the X and Z radii. Next, calculations were conducted for the experimental data itself ("actual") as well as the predicted values ("modeled"). Finally, two sets of statistics were collected. The first included the entire *area under the curve* for each shot

28

as a sum value. The benefit of such a value is that it allows for a simple ratio of how much actual area was predicted with the model. However, each shot had a different number of time steps. Using only the total area would mean that shots with more time steps would receive more weight than other shots. To compensate for this factor, statistics were also collected as an average for each shot. The sum of the *area under the curve* was divided by the number of time steps within a shot to receive an average area per time step of a shot. All of these calculations resulted in eight data points collected for each shot.

4.3. Sub-model Development

Taking the previous set of data points for each material type (98 for 7075 aluminum and 101 for 2024 aluminum), the sets were further broken down into two sets, as discussed earlier. Set A of 7075 aluminum had 48 shots while Set B had 50. For 2024 aluminum, Set A had 48 shots and Set B had 53. These four different sets of data were then run through the same Matlab .m script as described in Section 4.1 (page 21), and the following four models were developed:

	X-direction		Z-direction	
	β	γ	β	γ
velocity	1.63E-05	0.000187	-2.47E-05	0.00041
obliquity	-0.002926	0.021701	0.005122	0.009166
thickness	-1.46357	-3.76279	-1.16001	-6.98261
mass	0.0019083	0.010853	0.003038	0.011502
intercept	1.9453349	4.353412	1.749417	3.699419

Table 6: 7075 Aluminum Set A Model

	X-direction			Z-direction	
	β	γ		β	γ
velocity	1.41E-05	0.000405		-3.01E-05	0.000583
obliquity	-0.003035	0.02099		0.004706	0.006547
thickness	0.417437	2.135418		0.0467	0.114773
mass	0.0016317	0.010481		0.003247	0.011507
intercept	1.4888152	1.801211		1.441755	1.367277

Table 7: 7075 Aluminum Set B Model

	X-direction			Z-direction	
	β	γ		β	γ
velocity	1.00E-04	0.000401		3.14E-05	0.000692
obliquity	-0.00184	0.016322		0.004391	0.005343
thickness	1.683141	0.620028		1.260783	-3.41515
mass	0.001254	0.011902		0.002759	0.01059
intercept	0.755984	1.834589		0.899578	1.199265

Table 8: 2024 Aluminum Set A Model

	X-direction			Z-direction	
	β	γ		β	γ
velocity	1.56E-04	0.000496		8.01E-05	0.000781
obliquity	-0.00724	0.014227		0.001108	-0.00089
thickness	-0.9436	-1.48566		-0.33295	-3.46296
mass	0.003126	0.010495		0.002584	0.010584
intercept	0.917141	2.255132		1.059617	1.179727

Table 9: 2024 Aluminum Set B Model

For the most part, these two sets of models are similar. However, some key discrepancies exist. The coefficient for thickness changes signs between models from Set A to B for both 7075 aluminum and 2024 aluminum. Interestingly, they are negative for Set A of 7075 aluminum and Set B of 2024 aluminum, and positive for Set B of 7075 aluminum and Set A of 2024 aluminum. The beta column in the Z-direction for 2024 aluminum also has a discrepancy between Set A and Set B: the velocity coefficient is nearly three times smaller in Set A than Set B. Without knowing the confidence intervals on the

coefficients it is impossible to know how statistically different the numbers really are; however, they appear to be close enough to fairly accurate predict the other set of data. The confidence intervals were not calculated because as Henninger (2010) had discovered, the model error was not normally distributed, and therefore the error was not heavily analyzed.

4.4. Results

The various statistical methods were run in two main groups: the cross-validation comparing one set to the other, and an overall comparison of the models from each material type with the data from that material type. The validation results demonstrate that the overall models are valid.

4.4.1. Cross-validation

For each material type, the shots from Set A were predicted using the model developed from Set B, and vice versa. The goodness of these predictions was summarized using the R^2 statistic as well as MSE. A snapshot of the results is summarized in Table 10, while the complete results can be found in the accompanying spreadsheet under the tab "Stats_R2_MSE". The table has several columns. The first designates the shot corresponding to that row of statistics. The 2nd, 4th, and 6th columns correspond to calculations regarding the radius in the X-direction while the 3rd, 5th, and 7th columns correspond to calculations regarding the Z-direction. The 2nd and 3rd columns correspond to the R^2 value, as calculated by Equation 10. The 4th and 5th columns correspond to the R_0^2 value, as calculated in Equation 11. The final two columns correspond to the Mean Square error (MSE) as calculated in Equation 12.

Shot	R^2_x	R^2_z	$R_o^2\_x$	$R_o^2\_z$	MSE_x	MSE_z
T047R	1.39	0.76	-0.53	0.06	808.37	2511.17
T058R	0.57	1.07	0.07	-0.33	120.64	920.39
T094R	4.23	1.62	-2.37	0.07	612.69	912.97
T117R	1.07	0.56	-1.14	-0.05	243.97	285.57
T143R	0.22	4.29	-0.47	-4.14	187.71	351.06
T147R	139.80	0.25	-137.79	0.27	435.43	31.81
T156	0.69	0.69	0.47	0.56	602.04	1172.60
T166R	33.65	1.68	-32.68	-0.98	1313.77	2854.75
T316R	0.97	13.39	0.83	-10.35	5.49	30.05
T324R	0.55	0.75	0.68	0.92	228.65	151.82
T047R	1.39	0.76	-0.53	0.06	808.37	2511.17
T058R	0.57	1.07	0.07	-0.33	120.64	920.39

Table 10: Snapshot of 2024 Set A Model Results

The resulting values for R^2 are very disturbing. In general, such values should range between zero and one. Clearly the above results do not follow this trend, as the R^2 reaches as high as 139.80 for shot T147R. The equations for R^2 assume that the values follow the *fundamental analysis-of-variance identity for a regression model*. This identity states that the sum of squares total is equal to the additions of the sum of squares from the regression and the residual sum of square (Montgomery, Peck, & Vining, 2006, p. 26). In many of these cases, this fundamental identity fails. For example, shot T147R has the following parameters for the radius in the x direction: $SS_{err} = 2177$, $SS_{reg} = 2193$, $SS_{tot} = 16$. Clearly $2177+2193\neq16$. Consequentially, the resulting R^2 values have no worthwhile meaning. As discussed earlier, the MSE values are also extremely hard to interpret as even this small sample range from 5 to 2855. While the values can be compared against each other to see points that were predicted better than others, it cannot be immediately known if the larger values are still very good or if they are terrible. This lack of insight led to using the *area under the curve* measure.

For this set of statistics, a separate matlab .m file was written. As explained in section 4.2.3, the code steps through each shot and adds the radii together, since the area is represented by the radii times a time step of one. This value is recorded, as well as the average of each time step within a shot. The code allows for various combinations of models and set data, and it outputs the resulting areas. These numbers were then transferred into an excel spreadsheet. Each shot was then matched up with its corresponding design point (based upon its input parameters of target velocity, obliquity angle, panel thickness, and frag size). The 32 design points are shown in the table below:

	Vel	Angle	Thick	Mass		Vel	Angle	Thick	Mass
1	4000	0	0.063	20	17	7000	0	0.063	20
2	4000	0	0.063	40	18	7000	0	0.063	40
3	4000	0	0.063	75	19	7000	0	0.063	75
4	4000	0	0.063	150	20	7000	0	0.063	150
5	4000	0	0.25	20	21	7000	0	0.25	20
6	4000	0	0.25	40	22	7000	0	0.25	40
7	4000	0	0.25	75	23	7000	0	0.25	75
8	4000	0	0.25	150	24	7000	0	0.25	150
9	4000	45	0.063	20	25	7000	45	0.063	20
10	4000	45	0.063	40	26	7000	45	0.063	40
11	4000	45	0.063	75	27	7000	45	0.063	75
12	4000	45	0.063	150	28	7000	45	0.063	150
13	4000	45	0.25	20	29	7000	45	0.25	20
14	4000	45	0.25	40	30	7000	45	0.25	40
15	4000	45	0.25	75	31	7000	45	0.25	75
16	4000	45	0.25	150	32	7000	45	0.25	150

Table 11: Design Points

The averages of each shot within a design parameter were then taken to give a resulting area and average area for each direction, actual and modeled, for each design point. A graph was then developed for each model comparison of design point versus area.

33

The following pages show figures which demonstrate the various results from the cross validation calculations. In order to determine a general goodness of fit, the eyeball test was used. In other words, the graphs were viewed to determine how closely the model predicted the actual data. This information is also coupled with the MSE for each shot. The reason for this is that the graphs simply show the average areas between various shots. If the model overestimated for one shot and underestimated it for another, then the graph would show a good fit despite the fact that the many errors existed. When coupled with MSE, a high MSE with a good graph implies this phenomenon occurred while a low MSE implies the model was in fact accurate.
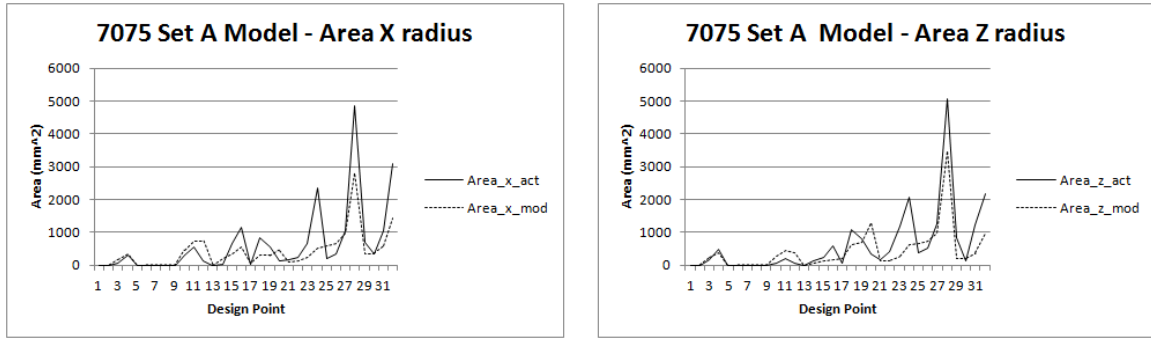
Figure 4: 7075 Set A Model Cumulative Area

This figure shows the results from running the data from 7075 aluminum Set B into the model developed using data from Set A of 7075 aluminum and looking at the total area. The modeled line follows the actual line quite closely. Point 24 has the biggest discrepancy: this occurs when the velocity, thickness, and fragment grain size are all at their highest settings.
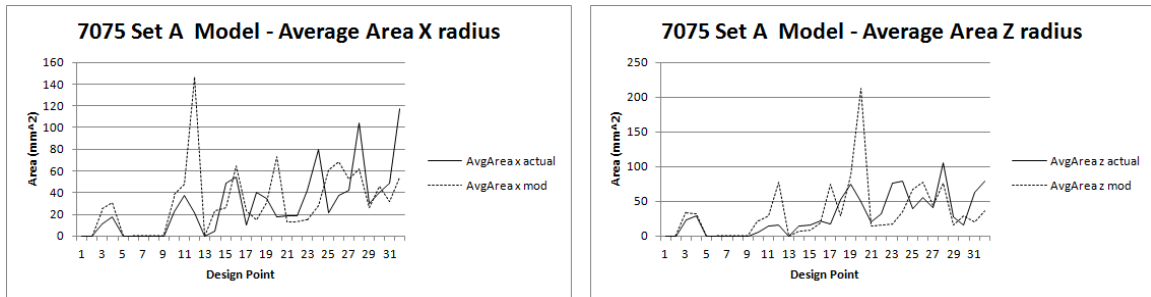
Figure 5: 7075 Set A Model Average Area

This figure is from the same data set as above. The difference is that this figure takes the average area for each shot as opposed to the cumulative area. There is more discrepancy in these models than in the straight area, but in general model still follows the actual data fairly well. The biggest point of concern involves point 12 with the X radius and point 20 in the Z radius. Both of these points involve cases where the fragment size is 150 grains.
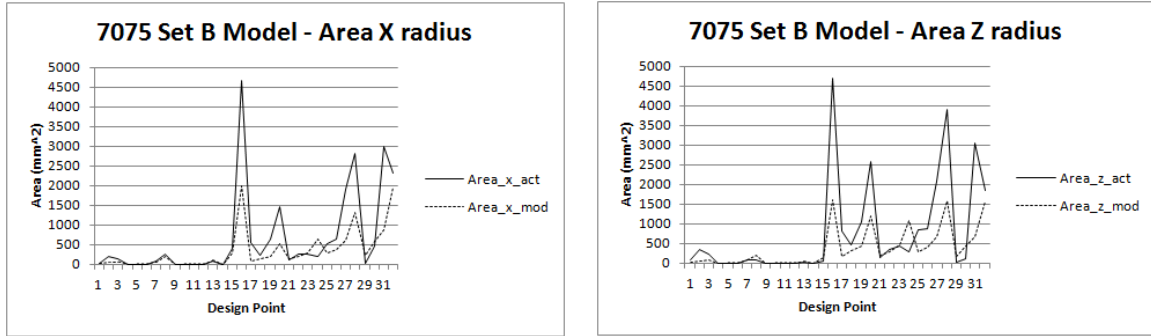
Figure 6: 7075 Set B Model Cumulative Area

This figure uses the data from Set A applied to the model developed using Set B, again from 7075 aluminum. The modeled line closely follows the actual line, with a couple key discrepancies. The model from points 16, 20, and 28 under-predicted the area when compared to the actual area. All three of these points involve parameters where the fragment size is 150 grains.
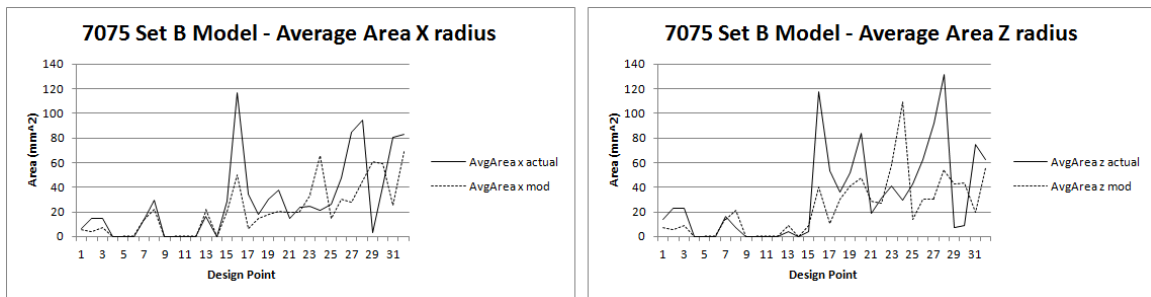
Figure 7: 7075 Set B Model Average Area

Similarly to the previous figures from the 7075 aluminum data, the average area models appear to predict the actual data, although they do so less accurately than the cumulative area models. The model from points 16 and 28 under-predicted the area when compared to the actual area. The model from points 24 and 29 over-predicted the area when compared to the actual area. Data points 16, 24, and 28 each involved parameters where the fragment size is 150 grains.

36
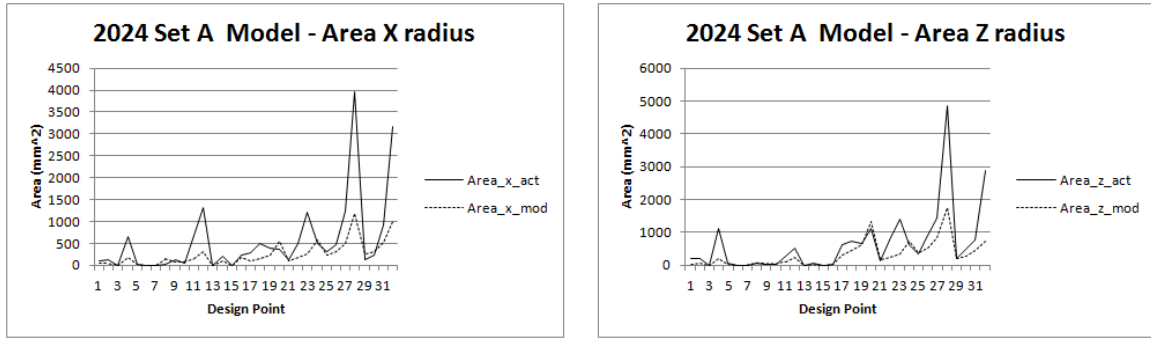
Figure 8: 2024 Set A Model Cumulative Area

This figure uses the data from the 2024 aluminum where the Set B data was inserted into the model developed using the Set A data. The modeled line closely follows the actual line, with a couple key discrepancies. The model from points 12, 23, 28, and 32 under-predicted the area when compared to the actual area in the X direction, while the points 4, 23, 28, and 32 under-predicted the area when compared to the actual area in the Z direction. The three even points involve parameters where the fragment size is 150 grains, and point 23 has input parameters of high velocity and thickness, and a fragment size of 75 grains.
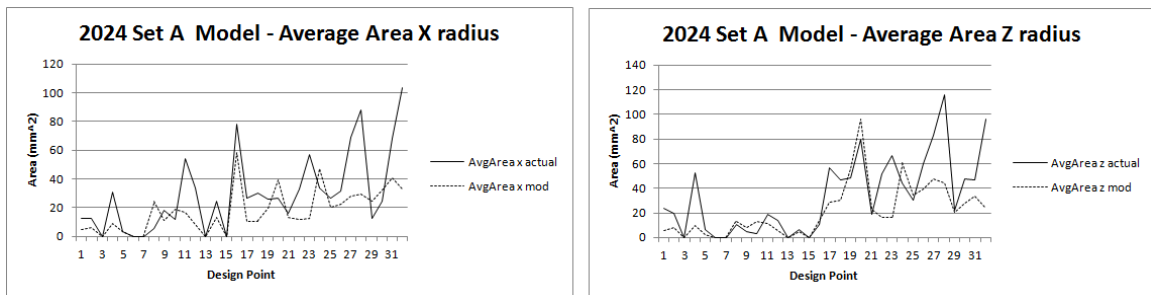
Figure 9: 7075 Set A Model Average Area

Similar to the 7075 aluminum models, the average area is a little more sporadic but still a generally good fit. The largest discrepancies occur with points 4, 11, 12, 23, 28 and 32. All of these points involve larger fragment sizes, with points 4, 12, 28, and 32 containing fragment sizes of 150 grains while points 11 and 23 have a fragment size of 75 grains.

37
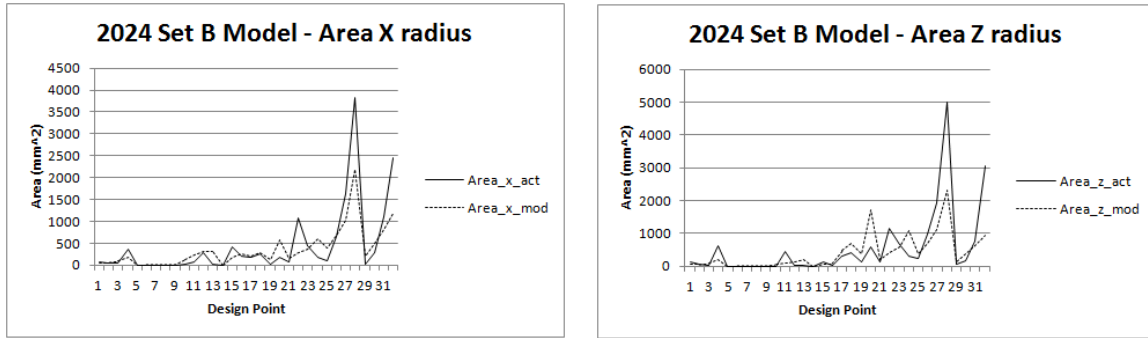
Figure 10: 2024 Set B Model Cumulative Area

This table takes the data from 2024 aluminum Set A and testing it against the model developed using the data from Set B. The modeled line closely follows the actual line, with a couple key discrepancies. The model from points 22, 28, and 32 under-predicted the area when compared to the actual area in both the X and Z directions. Point 20 over-predicts the area in the Z direction. Points 20, 28, and 32 have fragment sizes of 150 grains. Point 22 has a high velocity, high thickness, and a fragment size of 40 grains.
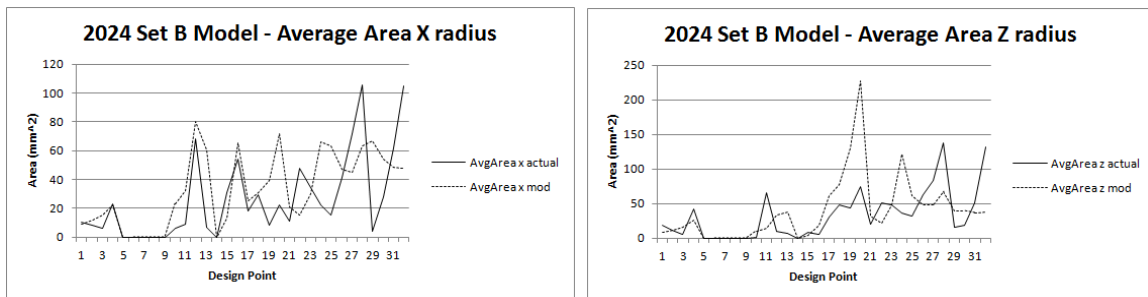
Figure 11: 7075 Set A Model Average Area

The average area graphs generally model the actual data well, with a few discrepancies. Points 28 and 32 under-predict the area when compared to the actual area in both the X and Z directions. Points 20, 24, 25, 29 over-predict the area when compared to the actual area in the X direction, with the same phenomena occurring with points 20 and 24 in the Z direction. Again, points 20, 24, 28, and 32 have fragment sizes of 150 grains, while points 25 and 29 are the only issues with fragment sizes of 20 grains.

The previous figures show the results from the cross-validation. As discussed under each figure, for the most part the model predicted the data very well. The key differences occurred most often at points which involved a fragment size of 150 grains. This phenomena shows that while the model overall does a good job of predicting the data, it clearly does not compensate enough for a large fragment size. Interestingly, the data from points 28 and 32 which appeared to cause the most issues did not correlate to the highest MSE values. While the science is not perfect, this method still gives the analyst confidence that the models are valid.

4.4.2. Final Model Validation

The same analysis technique used for the cross-validation was used for the full models for each material type. It would be expected that these models would show that they predict the values better than the models from each set because each data point that is being predicted was used to develop the model. However, since the two different sets did a good job of predicting the other, the full models should be similarly accurate. The following figures are the results of the models using the full data set for each type of aluminum, again broken into charts for X and Z directions as well as cumulative area and average area.
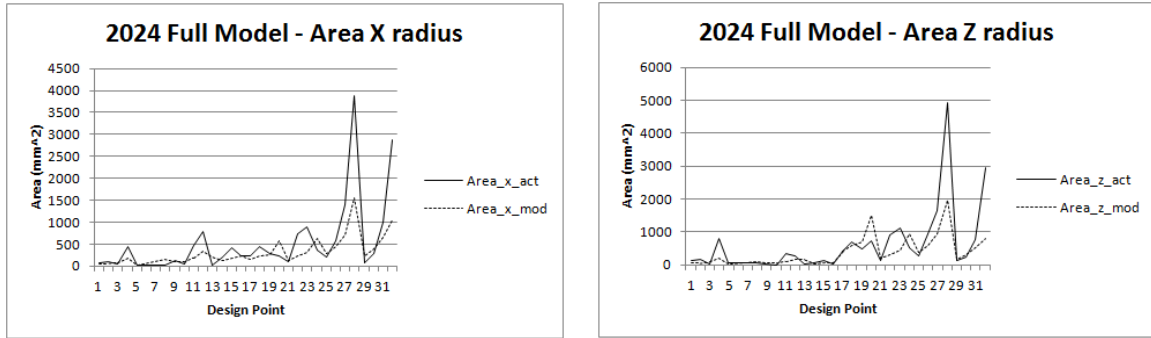
Figure 12: 2024 Full Model Cumulative Area

This figure comes from the full 2024 aluminum model. As expected, it appears to predict the area extremely well. Once again, the big discrepancies occur at points 28 and 32, where the velocity is set at high and the fragment size is at its largest.
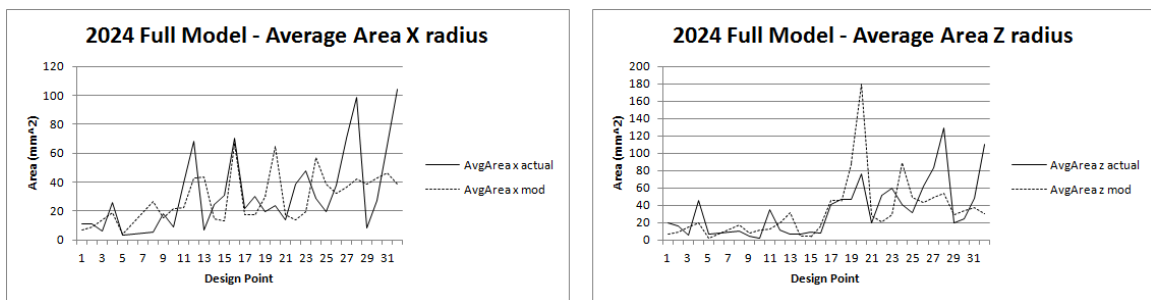
Figure 13: 2024 Full Model Average Area

The average area seems to be a little more sporadic than would be expected with data being run into a model that had the same data used to develop it. However, looking at how sporadic the actual data itself appear, it is not surprising that the model cannot match it exactly. Similar to past results, the biggest discrepancies appear to be at points 20, 28, and 32 in both charts. This further emphasizes the fact that the model has some issues with larger fragment sizes.
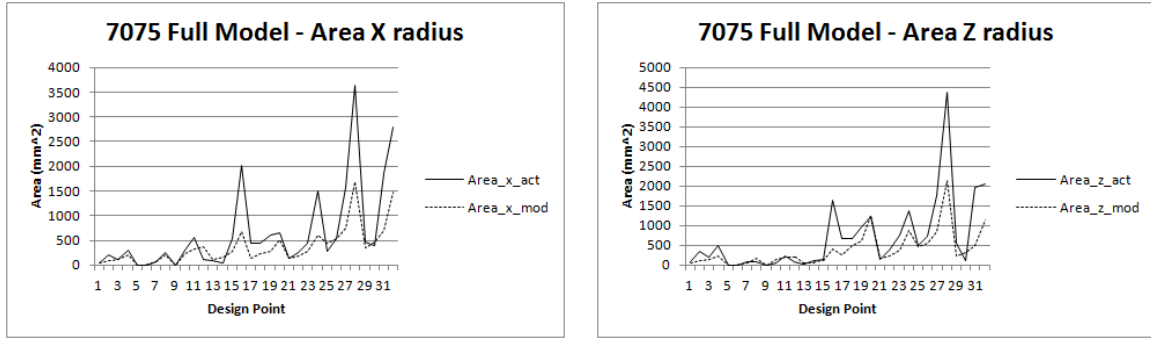
Figure 14: 7075 Full Model Cumulative Area

The results from 7075 aluminum appear extremely similar to those from 2024 aluminum. The discrepancies occur at points 16, 28, and 32 in both directions as well as point 24 in the X direction. These points maintain the common trend that the model has a difficult time accurately predicting the flashes with large fragment sizes.
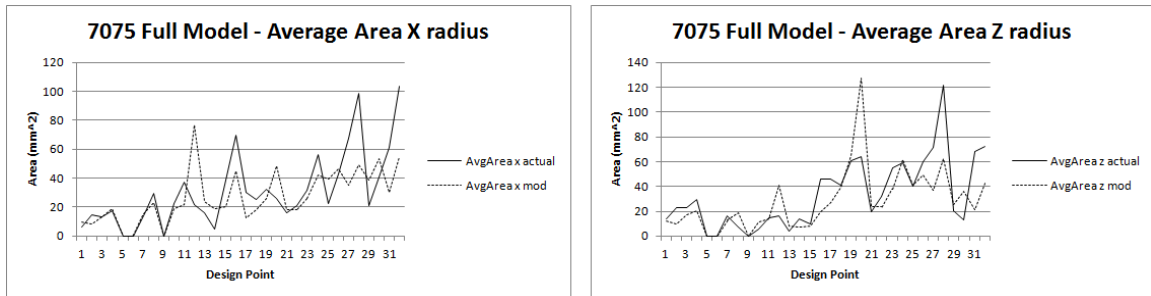
Figure 15: 7075 Full Model Average Area

As with the previous figures, the average models do not predict as closely as the cumulative models did. However, they still appear quite accurate. The largest discrepancies occur at points 12, 28, and 32 in both directions and point 20 in the Z direction. All four of these data points involve a fragment size of 150 grains, further supporting the issue that the models have with regard to large fragment sizes.

4.5. Future Studies

Overall, the provided models accurately predict flashes, given they occur, for input parameters within the ranges of those collected for this study. However, there are certain areas which can be further explored to improve upon this work. The first piece involves the coefficients with regard to the penetrator size. In many of the validations, the main design parameters with issues involved parameters where the penetrator size was 150 grains. Perhaps one cause is that the regression does not take the appropriate non-linear approach.

As discussed, these models are based upon shots where the penetrator was a fragment. Similar tests could be run with actual rounds to see if the models still hold true; if not, the same methodology used in this research could be applied to penetrator rounds to develop new models. In addition, these models cover a fairly limited range of their parameters. Perhaps data within these ranges could further validate the model, or perhaps input parameters beyond the current ranges could be included to further aid the robustness of the models.

Finally, the 46th Test Group, Survivability Analysis Flight has discussed the desire to have a final model which not only predicts the size of the flash, but also its intensity. Such a model would require further testing and data recording, as well as someone who understands the physical properties associated with heat transfer. However, combining those efforts with this model would further help the Survivability Analysis Flight achieve their final goal.

5.   Conclusions

Aircrew members flying combat missions, as well as those associated with these aircrews, are concerned with the chance that a fragment from an exploding device may penetrate into the airframe and cause a *flash* which could possibly ignite a fire onboard that aircraft. Being able to understand and model a flash based upon input parameters is extremely important because if an accurate model is known, then cases which provide high chances of a fire can be further analyzed and negated. Continuing past research, this thesis looks at the penetration of a fragment through a material as well as the back-face flash. It considers the current way penetration is predicted, provides an initial look at the chances of having a flash given a penetration occurs, and provides a model to predict the back-face flash with respect to time assuming that a flash occurs. The data used for this research was provided by the sponsor of the research, the 46th Test Group, Survivability Analysis Flight.

Chapter 3 considered the penetration aspect of the research. It used the program FATEPEN to predict whether or not a penetration should have occurred for the data; the results indicated every shot should have penetrated the target, and this fact was validated. Since no model existed to determine the likelihood of a back-face flash given that a penetration occurred, simple percentages were taken of the available data to give a general idea of which factors affected the existence of a back-face flash, and an initial model was developed.

Chapter 4 provided the framework for the meta-models for a back-face flash over time. Models were developed for sets of the overall data in order to allow cross-validation. The statistical methods to perform such validations were discussed and the

results were provided. The final meta-models were also provided, as well as a validation of these final models.

This thesis lays a foundation for further work. While it provides an initial model for predicting the existence of a back-face flash given that a penetration occurs, the model needs much more analysis and improvement. The current model, while accurate, constantly had issues with an input parameter of the largest penetrator size. Further look into this phenomenon would result in a more accurate model. Similarly, the model could be expanded to include a wider range of input parameters. A heat intensity addition could be made, further approaching the sponsor's final goal.

Appendix A: Design Parameters

Std	Test No.	Velocity (fps)	Obliquity (deg)	Material Type	Thickness (in)	Frag Size (grain)
221	31	4000	0	7075 T651	0.25	75
186	32	7000	0	7075 T6	0.063	75
306	33	7000	0	7075 T651	0.25	150
146	34	7000	0	7075 T651	0.25	40
201	35	4000	0	2024 T351	0.25	75
66	36	7000	0	7075 T651	0.25	20
106	37	7000	0	7075 T6	0.063	40
241	38	4000	0	2024 T3	0.063	150
181	39	4000	0	7075 T6	0.063	75
246	40	7000	0	2024 T3	0.063	150
1	41	4000	0	2024 T3	0.063	20
141	42	4000	0	7075 T651	0.25	40
301	43	4000	0	7075 T651	0.25	150
281	44	4000	0	2024 T351	0.25	150
286	45	7000	0	2024 T351	0.25	150
266	46	7000	0	7075 T6	0.063	150
206	47	7000	0	2024 T351	0.25	75
6	48	7000	0	2024 T3	0.063	20
166	49	7000	0	2024 T3	0.063	75
161	50	4000	0	2024 T3	0.063	75
261	51	4000	0	7075 T6	0.063	150
41	52	4000	0	2024 T351	0.25	20
46	53	7000	0	2024 T351	0.25	20
26	54	7000	0	7075 T6	0.063	20
226	55	7000	0	7075 T651	0.25	75
121	56	4000	0	2024 T351	0.25	40
86	57	7000	0	2024 T3	0.063	40
126	58	7000	0	2024 T351	0.25	40
61	59	4000	0	7075 T651	0.25	20
81	60	4000	0	2024 T3	0.063	40
101	61	4000	0	7075 T6	0.063	40
21	62	4000	0	7075 T6	0.063	20
307	63	7000	0	7075 T651	0.25	150
67	64	7000	0	7075 T651	0.25	20
122	65	4000	0	2024 T351	0.25	40
102	66	4000	0	7075 T6	0.063	40
222	67	4000	0	7075 T651	0.25	75
107	68	7000	0	7075 T6	0.063	40
202	69	4000	0	2024 T351	0.25	75
167	70	7000	0	2024 T3	0.063	75
242	71	4000	0	2024 T3	0.063	150

45

Std	Test No.	Velocity (fps)	Obliquity (deg)	Material Type	Thickness (in)	Frag Size (grain)
147	72	7000	0	7075 T651	0.25	40
2	73	4000	0	2024 T3	0.063	20
247	74	7000	0	2024 T3	0.063	150
7	75	7000	0	2024 T3	0.063	20
42	76	4000	0	2024 T351	0.25	20
262	77	4000	0	7075 T6	0.063	150
302	78	4000	0	7075 T651	0.25	150
142	79	4000	0	7075 T651	0.25	40
87	80	7000	0	2024 T3	0.063	40
267	81	7000	0	7075 T6	0.063	150
182	82	4000	0	7075 T6	0.063	75
82	83	4000	0	2024 T3	0.063	40
47	84	7000	0	2024 T351	0.25	20
207	85	7000	0	2024 T351	0.25	75
22	86	4000	0	7075 T6	0.063	20
162	87	4000	0	2024 T3	0.063	75
62	88	4000	0	7075 T651	0.25	20
227	89	7000	0	7075 T651	0.25	75
187	90	7000	0	7075 T6	0.063	75
127	91	7000	0	2024 T351	0.25	40
282	92	4000	0	2024 T351	0.25	150
27	93	7000	0	7075 T6	0.063	20
287	94	7000	0	2024 T351	0.25	150
163	95	4000	0	2024 T3	0.063	75
28	96	7000	0	7075 T6	0.063	20
188	97	7000	0	7075 T6	0.063	75
88	98	7000	0	2024 T3	0.063	40
83	99	4000	0	2024 T3	0.063	40
43	100	4000	0	2024 T351	0.25	20
103	101	4000	0	7075 T6	0.063	40
143	102	4000	0	7075 T651	0.25	40
23	103	4000	0	7075 T6	0.063	20
283	104	4000	0	2024 T351	0.25	150
148	105	7000	0	7075 T651	0.25	40
208	106	7000	0	2024 T351	0.25	75
108	107	7000	0	7075 T6	0.063	40
243	108	4000	0	2024 T3	0.063	150
303	109	4000	0	7075 T651	0.25	150
123	110	4000	0	2024 T351	0.25	40
308	111	7000	0	7075 T651	0.25	150
128	112	7000	0	2024 T351	0.25	40
223	113	4000	0	7075 T651	0.25	75

Std	Test No.	Velocity (fps)	Obliquity (deg)	Material Type	Thickness (in)	Frag Size (grain)
268	114	7000	0	7075 T6	0.063	150
3	115	4000	0	2024 T3	0.063	20
8	116	7000	0	2024 T3	0.063	20
48	117	7000	0	2024 T351	0.25	20
63	118	4000	0	7075 T651	0.25	20
228	119	7000	0	7075 T651	0.25	75
163	120	4000	0	7075 T6	0.063	150
68	121	7000	0	7075 T651	0.25	20
248	122	7000	0	2024 T3	0.063	150
168	123	7000	0	2024 T3	0.063	75
183	124	4000	0	7075 T6	0.063	75
288	125	7000	0	2024 T351	0.25	150
203	126	4000	0	2024 T351	0.25	75
44	127	4000	0	2024 T351	0.25	20
269	128	7000	0	7075 T6	0.063	150
69	129	7000	0	7075 T651	0.25	20
169	130	7000	0	2024 T3	0.063	75
144	131	4000	0	7075 T651	0.25	40
24	132	4000	0	7075 T6	0.063	20
129	133	7000	0	2024 T351	0.25	40
209	134	7000	0	2024 T351	0.25	75
204	135	4000	0	2024 T351	0.25	75
244	136	4000	0	2024 T3	0.063	150
4	137	4000	0	2024 T3	0.063	20
84	138	4000	0	2024 T3	0.063	40
184	139	4000	0	7075 T6	0.063	75
264	140	4000	0	7075 T6	0.063	150
169	141	7000	0	7075 T651	0.25	40
29	142	7000	0	7075 T6	0.063	20
49	143	7000	0	2024 T351	0.25	20
64	144	4000	0	7075 T651	0.25	20
189	145	7000	0	7075 T6	0.063	75
249	146	7000	0	2024 T3	0.063	150
284	147	4000	0	2024 T351	0.25	150
109	148	7000	0	7075 T6	0.063	40
304	149	4000	0	7075 T651	0.25	150
9	150	7000	0	2024 T3	0.063	20
309	151	7000	0	7075 T651	0.25	150
89	152	7000	0	2024 T3	0.063	40
104	153	4000	0	7075 T6	0.063	40
224	154	4000	0	7075 T651	0.25	75
164	155	4000	0	2024 T3	0.063	75

Std	Test No.	Velocity (fps)	Obliquity (deg)	Material Type	Thickness (in)	Frag Size (grain)
289	156	7000	0	2024 T351	0.25	150
124	157	4000	0	2024 T351	0.25	40
229	158	7000	0	7075 T651	0.25	75
50	159	7000	0	2024 T351	0.25	20
110	160	7000	0	7075 T6	0.063	40
145	161	4000	0	7075 T651	0.25	40
170	162	7000	0	2024 T3	0.063	75
90	163	7000	0	2024 T3	0.063	40
85	164	4000	0	2024 T3	0.063	40
70	165	7000	0	7075 T651	0.25	20
130	166	7000	0	2024 T351	0.25	40
105	167	4000	0	7075 T6	0.063	40
25	168	4000	0	7075 T6	0.063	20
250	169	7000	0	2024 T3	0.063	150
185	170	4000	0	7075 T6	0.063	75
146	171	4000	0	2024 T3	0.063	40
30	172	7000	0	7075 T6	0.063	20
205	173	4000	0	2024 T351	0.25	75
285	174	4000	0	2024 T351	0.25	150
230	175	7000	0	7075 T651	0.25	75
225	176	4000	0	7075 T651	0.25	75
270	177	7000	0	7075 T6	0.063	150
150	178	7000	0	7075 T651	0.25	40
245	179	4000	0	2024 T3	0.063	150
125	180	4000	0	2024 T351	0.25	40
190	181	7000	0	7075 T6	0.063	75
45	182	4000	0	2024 T351	0.25	20
10	183	7000	0	2024 T3	0.063	20
265	184	4000	0	7075 T6	0.063	150
310	185	7000	0	7075 T651	0.25	150
210	186	7000	0	2024 T351	0.25	75
65	187	4000	0	7075 T651	0.25	20
305	188	4000	0	7075 T651	0.25	150
290	189	7000	0	2024 T351	0.25	150
5	190	4000	0	2024 T3	0.063	20
116	191	7000	45	7075 T6	0.063	40
56	192	7000	45	2024 T351	0.25	20
211	193	4000	45	2024 T351	0.25	75
311	194	4000	45	7075 T651	0.25	150
11	195	4000	45	2024 T3	0.063	20
296	196	7000	45	2024 T351	0.25	150
196	197	7000	45	7075 T6	0.063	75

Std	Test No.	Velocity (fps)	Obliquity (deg)	Material Type	Thickness (in)	Frag Size (grain)
276	198	7000	45	7075 T6	0.063	150
51	199	4000	45	2024 T351	0.25	20
151	200	4000	45	7075 T651	0.25	40
176	201	7000	45	2024 T3	0.063	75
291	202	4000	45	2024 T351	0.25	150
271	203	4000	45	7075 T6	0.063	150
16	204	7000	45	2024 T3	0.063	20
111	205	4000	45	7075 T6	0.063	40
216	206	7000	45	2024 T351	0.25	75
91	207	4000	45	2024 T3	0.063	40
191	208	4000	45	7075 T6	0.063	75
231	209	4000	45	7075 T651	0.25	75
171	210	4000	45	2024 T3	0.063	75
236	211	7000	45	7075 T651	0.25	75
316	212	7000	45	7075 T651	0.25	150
256	213	7000	45	2024 T3	0.063	150
156	214	7000	45	7075 T651	0.25	40
96	215	7000	45	2024 T3	0.063	40
131	216	4000	45	2024 T351	0.25	40
251	217	4000	45	2024 T3	0.063	150
71	218	4000	45	7075 T651	0.25	20
76	219	7000	45	7075 T651	0.25	20
31	220	4000	45	7075 T6	0.063	20
36	221	7000	45	7075 T6	0.063	20
136	222	7000	45	2024 T351	0.25	40
277	223	7000	45	7075 T6	0.063	150
32	224	4000	45	7075 T6	0.063	20
37	225	7000	45	7075 T6	0.063	20
57	226	7000	45	2024 T351	0.25	20
177	227	7000	45	2024 T3	0.063	75
257	228	7000	45	2024 T3	0.063	150
17	229	7000	45	2024 T3	0.063	20
92	230	4000	45	2024 T3	0.063	40
112	231	4000	45	7075 T6	0.063	40
197	232	7000	45	7075 T6	0.063	75
137	233	7000	45	2024 T351	0.25	40
252	234	4000	45	2024 T3	0.063	150
292	235	4000	45	2024 T351	0.25	150
297	236	7000	45	2024 T351	0.25	150
152	237	4000	45	7075 T651	0.25	40
217	238	7000	45	2024 T351	0.25	75
232	239	4000	45	7075 T651	0.25	75

Std	Test No.	Velocity (fps)	Obliquity (deg)	Material Type	Thickness (in)	Frag Size (grain)
192	240	4000	45	7075 T6	0.063	75
97	241	7000	45	2024 T3	0.063	40
157	242	7000	45	7075 T651	0.25	40
72	243	4000	45	7075 T651	0.25	20
132	244	4000	45	2024 T351	0.25	40
317	245	7000	45	7075 T651	0.25	150
52	246	4000	45	2024 T351	0.25	20
12	247	4000	45	2024 T3	0.063	20
272	248	4000	45	7075 T6	0.063	150
312	249	4000	45	7075 T651	0.25	150
117	250	7000	45	7075 T6	0.063	40
77	251	7000	45	7075 T651	0.25	20
212	252	4000	45	2024 T351	0.25	75
172	253	4000	45	2024 T3	0.063	75
237	254	7000	45	7075 T651	0.25	75
53	255	4000	45	2024 T351	0.25	20
153	256	4000	45	7075 T651	0.25	40
173	257	4000	45	2024 T3	0.063	75
213	258	4000	45	2024 T351	0.25	75
138	259	7000	45	2024 T351	0.25	40
158	260	7000	45	7075 T651	0.25	40
93	261	4000	45	2024 T3	0.063	40
298	262	7000	45	2024 T351	0.25	150
98	263	7000	45	2024 T3	0.063	40
273	264	4000	45	7075 T6	0.063	150
13	265	4000	45	2024 T3	0.063	20
58	266	7000	45	2024 T351	0.25	20
178	267	7000	45	2024 T3	0.063	75
113	268	4000	45	7075 T6	0.063	40
178	269	7000	45	7075 T651	0.25	20
133	270	4000	45	2024 T351	0.25	40
38	271	7000	45	7075 T6	0.063	20
313	272	4000	45	7075 T651	0.25	150
258	273	7000	45	2024 T3	0.063	150
253	274	4000	45	2024 T3	0.063	150
193	275	4000	45	7075 T6	0.063	75
318	276	7000	45	7075 T651	0.25	150
218	277	7000	45	2024 T351	0.25	75
73	278	4000	45	7075 T651	0.25	20
198	279	7000	45	7075 T6	0.063	75
233	280	4000	45	7075 T651	0.25	75
278	281	7000	45	7075 T6	0.063	150

Std	Test No.	Velocity (fps)	Obliquity (deg)	Material Type	Thickness (in)	Frag Size (grain)
18	282	7000	45	2024 T3	0.063	20
238	283	7000	45	7075 T651	0.25	75
33	284	4000	45	7075 T6	0.063	20
118	285	7000	45	7075 T6	0.063	40
293	286	4000	45	2024 T351	0.25	150
314	287	4000	45	7075 T651	0.25	150
94	288	4000	45	2024 T3	0.063	40
254	289	4000	45	2024 T3	0.063	150
34	290	4000	45	7075 T6	0.063	20
79	291	7000	45	7075 T651	0.25	20
214	292	4000	45	2024 T351	0.25	75
199	293	7000	45	7075 T6	0.063	75
54	294	4000	45	2024 T351	0.25	20
294	295	4000	45	2024 T351	0.25	150
134	296	4000	45	2024 T351	0.25	40
39	297	7000	45	7075 T6	0.063	20
19	298	7000	45	2024 T3	0.063	20
139	299	7000	45	2024 T351	0.25	40
159	300	7000	45	7075 T651	0.25	40
219	301	7000	45	2024 T351	0.25	75
259	302	7000	45	2024 T3	0.063	150
279	303	7000	45	7075 T6	0.063	150
114	304	4000	45	7075 T6	0.063	40
59	305	7000	45	2024 T351	0.25	20
299	306	7000	45	2024 T351	0.25	150
194	307	4000	45	7075 T6	0.063	75
74	308	4000	45	7075 T651	0.25	20
99	309	7000	45	2024 T3	0.063	40
239	310	7000	45	7075 T651	0.25	75
179	311	7000	45	2024 T3	0.063	75
174	312	4000	45	2024 T3	0.063	75
319	313	7000	45	7075 T651	0.25	150
234	314	4000	45	7075 T651	0.25	75
274	315	4000	45	7075 T6	0.063	150
14	316	4000	45	2024 T3	0.063	20
154	317	4000	45	7075 T651	0.25	40
119	318	7000	45	7075 T6	0.063	40
80	319	7000	45	7075 T651	0.25	20
55	320	4000	45	2024 T351	0.25	20
115	321	4000	45	7075 T6	0.063	40
95	322	4000	45	2024 T3	0.063	40
60	323	7000	45	2024 T351	0.25	20

Std	Test No.	Velocity (fps)	Obliquity (deg)	Material Type	Thickness (in)	Frag Size (grain)
100	324	7000	45	2024 T3	0.063	40
320	325	7000	45	7075 T651	0.25	150
200	326	7000	45	7075 T6	0.063	75
140	327	7000	45	2024 T351	0.25	40
135	328	4000	45	2024 T351	0.25	40
180	329	7000	45	2024 T3	0.063	75
20	330	7000	45	2024 T3	0.063	20
220	331	7000	45	2024 T351	0.25	75
120	332	7000	45	7075 T6	0.063	40
255	333	4000	45	2024 T3	0.063	150
75	334	4000	45	7075 T651	0.25	20
300	335	7000	45	2024 T351	0.25	150
155	336	4000	45	7075 T651	0.25	40
280	337	7000	45	7075 T6	0.063	150
195	338	4000	45	7075 T6	0.063	75
15	339	4000	45	2024 T3	0.063	20
35	340	4000	45	7075 T6	0.063	20
235	341	4000	45	7075 T651	0.25	75
315	342	4000	45	7075 T651	0.25	150
40	343	7000	45	7075 T6	0.063	20
295	344	4000	45	2024 T351	0.25	150
160	345	7000	45	7075 T651	0.25	40
240	346	7000	45	7075 T651	0.25	75
215	347	4000	45	2024 T351	0.25	75
175	348	4000	45	2024 T3	0.063	75
260	349	7000	45	2024 T3	0.063	150
275	350	4000	45	7075 T6	0.063	150

Appendix B: JMP Output for Initial Back-Face Flash Probability Model

Response Flash Material=2024
Whole Model
Actual by Predicted Plot

Flash Predicted P<.0001
RSq=0.46 RMSE=0.3047
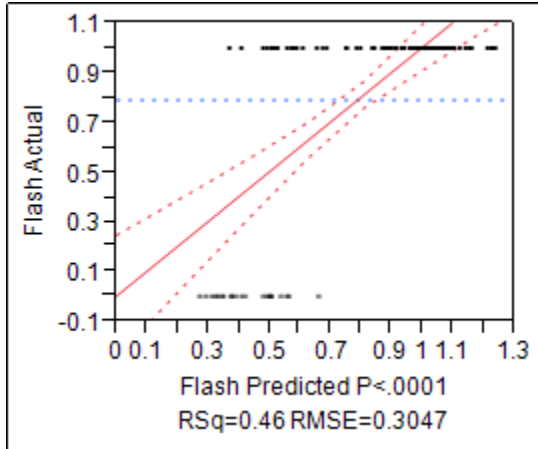
Summary of Fit

RSquare	0.464079
RSquare Adj	0.44665
Root Mean Square Error	0.304674
Mean of Response	0.789063
Observations (or Sum Wgts)	128

Residual by Predicted Plot

Flash Predicted
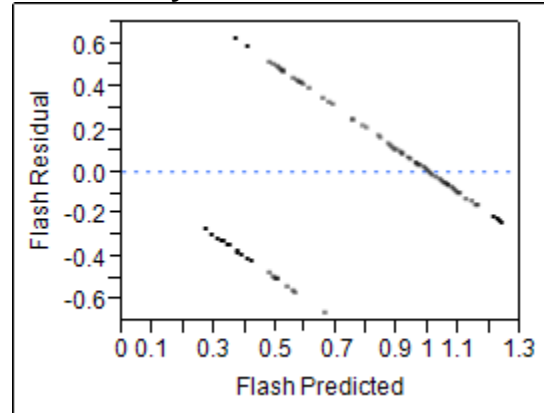
Analysis of Variance

Source	DF	Sum of Squares	Mean Square	F Ratio
Model	4	9.887049	2.47176	26.6278
Error	123	11.417638	0.09283	**Prob > F**
C. Total	127	21.304688		<.0001*

Lack Of Fit

Source	DF	Sum of Squares	Mean Square	F Ratio
Lack Of Fit	121	11.417638	0.094361	.
Pure Error	2	0.000000	0.000000	**Prob > F**
Total Error	123	11.417638		.
				Max RSq
				1.0000

Parameter Estimates

Term	Estimate	Std Error	t Ratio	Prob>|t|
Intercept	-0.052496	0.126841	-0.41	0.6797
Meas Vel	0.0001702	1.917e-5	8.88	<.0001*
Obliquity	-0.001731	0.00122	-1.42	0.1586
Thickness	-0.92642	0.288412	-3.21	0.0017*
Measured Size	0.001178	0.000559	2.11	0.0373*

 Above are the JMP results for the 2024 aluminum model. Looking at the parameter estimates, velocity, thickness, and penetrator size are all significant. However, there is a clear issue with the lack of fit since it accounts for 121 of the 123 degrees of freedom. Also, the residual vs predicted plot indicates non-constant variance. The data may need a transformation, or perhaps a response variable of "1" for a flash and "0" for no flash is not the best way to represent the data.
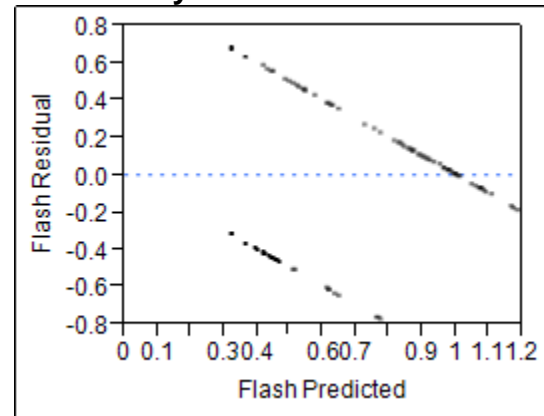
Response Flash Material=7075
Whole Model
Actual by Predicted Plot
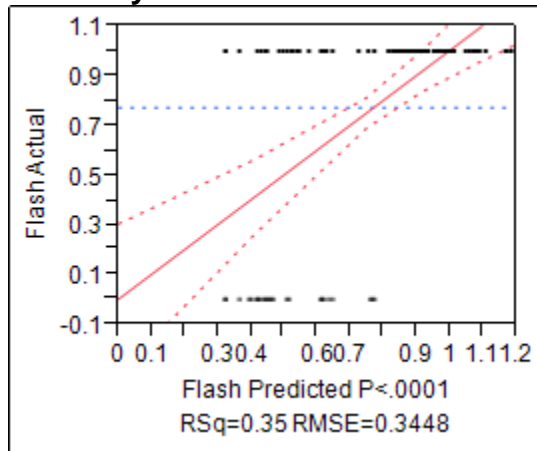
Summary of Fit

RSquare	0.351938
RSquare Adj	0.33069
Root Mean Square Error	0.344777
Mean of Response	0.771654
Observations (or Sum Wgts)	127

Residual by Predicted Plot

Analysis of Variance

Source	DF	Sum of Squares	Mean Square	F Ratio
Model	4	7.875644	1.96891	16.5634
Error	122	14.502308	0.11887	**Prob > F**
C. Total	126	22.377953		<.0001*

Lack Of Fit

Source	DF	Sum of Squares	Mean Square	F Ratio
Lack Of Fit	120	14.502308	0.120853	.
Pure Error	2	0.000000	0.000000	**Prob > F**
Total Error	122	14.502308		.
				Max RSq
				1.0000

Parameter Estimates

Term	Estimate	Std Error	t Ratio	Prob>|t|
Intercept	-0.118069	0.143087	-0.83	0.4109
Meas Vel	0.0001618	2.185e-5	7.40	<.0001*
Obliquity	-0.002054	0.001368	-1.50	0.1357
Thickness	-0.493729	0.329134	-1.50	0.1362
Measured Size	0.0014276	0.000611	2.34	0.0211*

Above are the JMP results for the 7075 aluminum model. Looking at the parameter estimates, velocity and penetrator size are both significant. However, there is a clear issue with the lack of fit since it accounts for 120 of the 122 degrees of freedom. Also, the residual vs predicted plot indicates non-constant variance. The data may need a transformation, or perhaps a response variable of "1" for a flash and "0" for no flash is not the best way to represent the data.
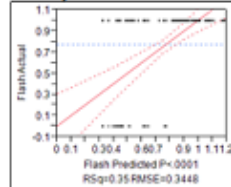
55

Ballistic Flash Characterization: Penetration and Back-Face Flash

2nd Lt Michael J. Koslow
Advisor: Dr. Raymond Hill
Readers: LTC Daryl Ahner, Mr. Jaime Bestard
Department of Operational Sciences (ENS)
Air Force Institute of Technology
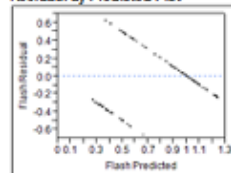Client: 46th Test Group, Survivability Analysis Flight

Penetration

- FATEPEN produced V50 values: velocity at which 50% chance of penetration
- All 255 usable shots had penetration
- Developed initial predication model in JMP to predict occurrence of back-face flash : messy results
  - Lack-of-fit and non-constant variance
- Calculated flash percentages based on input parameters: determined Velocity and Penetrator Size had greatest effect on back-face flash occurrence

Significance

- First-ever empirical boundary model characterizing ballistic impact flash for a back-face flash
- First look at predicting existence of back-face flash given input parameters
- Helps Client reach ultimate goal of model to predict flash size, duration, and heat intensity

Back-Face Flash

Factor	Variable	Levels	Units
Initial Velocity	Vel	4000, 7000	Feet/second
Obliquity Angle	Angle	0, 45	degrees
Material Type	Mat	AL2024, AL 7075	N/A
Panel Thickness	Thick	0.063, 0.25	inches
Penetrator Size	Mass	20,40,75,150	grains

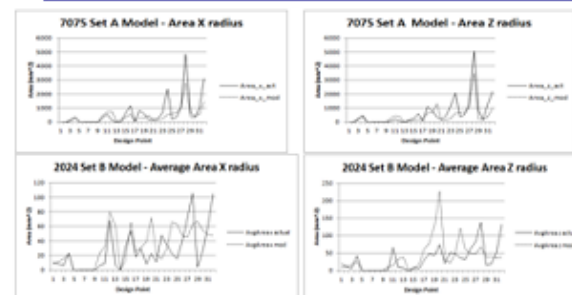Full-factorial design $(2^4 * 4^1)*5$ replications+30 calibration=350 shots

Meta-Model

$$Model\ Coefficient = e^{(b_0+b_1(vel)+b_2(oblq)+b_3(thick)+b_4(mass))}$$
$$FlashRadius(t) = \gamma \left(\left(\frac{\alpha}{\beta}\right)\left(\frac{t}{\beta}\right)^{(\alpha-1)} e^{-\left(\frac{t}{\beta}\right)}\right)$$

Results

Response Flash Material=7075
Whole Model
Actual by Predicted Plot

RSq=0.35 RMSE=0.3448

Residual by Predicted Plot

	Overall	% Flash
		78.04%
Target Velocity		
	4000	49.52%
	7000	98.00%
Obliquity		
	0	84.96%
	45	72.54%
Material		
	2024	79.53%
	7075	76.56%
Thickness		
	0.063	83.46%
	0.25	72.66%
Penetrator Size		
	20	63.64%
	40	75.38%
	75	84.75%
	150	89.23%

2024_Full

	X-direction		Z-direction	
	β	γ	β	γ
velocity	1.41E-04	0.000444	6.19E-05	0.000738
obliquity	-0.00435	0.014743	0.00267	0.001499
thickness	0.40562	-0.36829	0.456721	-3.2996
mass	0.001821	0.01093	0.002458	0.010505
intercept	0.775179	2.09957	0.959158	1.193209

7075_full

	X-direction		Z-direction	
	β	γ	β	γ
velocity	2.62E-05	0.000328	-2.08E-05	0.000527
obliquity	-0.00379	0.01852	0.004288	0.005618
thickness	-0.56001	-0.7615	-0.58819	-3.36013
mass	0.001419	0.009403	0.002938	0.010569
intercept	1.704262	3.039882	1.593113	2.468511

Cross-Validation

7075 Set A Model - Area X radius

7075 Set A Model - Area Z radius

2024 Set B Model - Average Area X radius

2024 Set B Model - Average Area Z radius

Bibliography

Ball, R. E. (2003). *The Fundamentals of Aircraft Combat Survivability Analysis and Design (Second Edition).* American Institute of Aeronautics and Astronautics.

Bestard, J. J., & Kocher, B. (2010). *Ballistic Impact Flash Characterization.* AIAA-2010-2573.

Blythe, R. M. (1993). *Preliminary Expirical Characterization of Steel Fragment Projectile Penetration of Graphite/Epoxy Composite and Aluminum Targets.* MS thesis, Air Force Insitute of Technology, Wright-Patterson AFB, Ohio.

Henninger, T. A. (2010). *Characterization of Ballistic Impact Flash: An Initial Investigation and Methods Development.* MS thesis, Air Force Institute of Technology, Wright-Patterson AFB, Ohio.

JTCG/ME. (1985, October 15). Penetration Equations Handbook for Kinetic-Energy Penetrators.

Knight, E. E. (1992). *Predicting Armor Piercing Incendiary Projectile Effects After Impacting Composite Material.* MS thesis, Air Force Institute of Technology, Wright-Patterson AFB, Ohio.

Lanning, J. W. (1993). *Predicting Armor Piercing Incendiary Projectile Effects After Impacting Two Composite Material.* MS thesis, Air Force Institute of Technology, Wright-Patterson AFB, Ohio.

Montgomery, D. C., Peck, E. A., & Vining, G. G. (2006). *Introduction to Linear Regression Analysis* (4th Edition ed.). Hoboken, New Jersey: Wiley-Interscience.

Peyton, D. J. (2012). *Ballistic Flash Characterization of Entry-Side Flash.* MS thesis, Air Force Institute of Technology, Wright-Patterson AFB, Ohio.

Reynolds, J. K. (1991). *A Response Surface Model for the Incendiary Functioning Characterizations of Soviet API Projectiles Impacting Graphite Epoxy Composite Panels.* MS thesis, Air Force Insitiute of Technology, Wright-Patterson AFB, Ohio.

SURVIAC. (n.d.). *Past Air Target Encounter PENetration Program*. Retrieved January 6, 2012, from Survivability/Vulnerability Information Analysis Center: http://www.bahdayton.com/surviac

Talafuse, T. P. (2011). *Empirical Characterization of Ballistic Impact Flash.* MS thesis, Air Force Institute of Technology, Wright-Patterson AFB, Ohio.

Vita

       Second Lieutenant Michael J. Koslow graduated from Springboro High School in Springboro, Ohio. He entered undergraduate studies at the United States Air Force Academy in Colorado Springs, Colorado where he graduated with a Bachelor of Science degree in Operations Research in May 2010. He received his commission and was recognized as a Distinguished Graduate.

       Although receiving a slot to Sheppard AFB for Euro-NATO Joint Jet Pilot Training, he decided to delay the training and take the Graduate Studies Program scholarship that was offered him by the Operations Research Department at the United States Air Force Academy. The scholarship gave him the chance to enter the Graduate School of Engineering and Management, Air Force Institute of Technology, in August 2010. In exchange, he receives the opportunity to teach at the United States Air Force Academy at a future point in his career. Upon graduation, he will be assigned to Sheppard AFB to attend Undergraduate Pilot Training.

REPORT DOCUMENTATION PAGE

The public reporting burden for this collection of information is estimated to average 1 hour per response, including the time for reviewing instructions, searching existing data sources, gathering and maintaining the data needed, and completing and reviewing the collection of information. Send comments regarding this burden estimate or any other aspect of the collection of information, including suggestions for reducing this burden to Department of Defense, Washington Headquarters Services, Directorate for Information Operations and Reports (0704-0188), 1215 Jefferson Davis Highway, Suite 1204, Arlington, VA 22202-4302. Respondents should be aware that notwithstanding any other provision of law, no person shall be subject to an penalty for failing to comply with a collection of information if it does not display a currently valid OMB control number.
PLEASE DO NOT RETURN YOUR FORM TO THE ABOVE ADDRESS.

1. REPORT DATE *(DD-MM-YYYY)*	2. REPORT TYPE	3. DATES COVERED *(From – To)*
22-03-2012	**Master's Thesis**	Sep 2010 - Mar 2012

4. TITLE AND SUBTITLE

Ballistic Flash Characterization:
Penetration and Back-Face Flash

5a. CONTRACT NUMBER

5b. GRANT NUMBER

5c. PROGRAM ELEMENT NUMBER

6. AUTHOR(S)

Koslow, Michael, J., Second Lieutenant, USAF

5d. PROJECT NUMBER

5e. TASK NUMBER

5f. WORK UNIT NUMBER

7. PERFORMING ORGANIZATION NAMES(S) AND ADDRESS(S)
Air Force Institute of Technology
Graduate School of Engineering and Management (AFIT/EN)
2950 Hobson Street, Building 642
WPAFB OH 45433-7765

8. PERFORMING ORGANIZATION REPORT NUMBER

AFIT-OR-MS-ENS-12-17

9. SPONSORING/MONITORING AGENCY NAME(S) AND ADDRESS(ES)
46th TG OL-AC
Attn: Mr. Jaime Bestard
2700 D Street, Bldg 1661   DSN: 785-6302 ext 231
WPAFB OH 45433   e-mail: Jaime.Bestard@wpafb.af.mil

10. SPONSOR/MONITOR'S ACRONYM(S)

11. SPONSOR/MONITOR'S REPORT NUMBER(S)

12. DISTRIBUTION/AVAILABILITY STATEMENT
        Distribution Statement A: APPROVED FOR PUBLIC RELEASE; DISTRIBUTION UNLIMITED.

13. SUPPLEMENTARY NOTES

14. ABSTRACT

        The Air Force is extremely concerned with the safety of its people, especially those who are flying aircraft. Onboard fires caused by munitions fire present a very real and dangerous threat. In order to help negate these incidents, analysts must be able to predict the flash that can occur when a projectile strikes a target. This thesis extends past AFIT research in developing a model to characterize a back-face flash, given a fragment penetration and a back-face flash occurs.

        The methodology in this research directly continues AFIT work for the 46th Test Group, Survivability Analysis Flight. It examines models to predict penetration of a fragment fired at a target and provides a first glance at an empirically-based likelihood of a penetration. Empirical live-fire fragment test data are used to create an empirical model of a flash event. The data are used to conduct statistical validation efforts. The resulting model provides an initial back-face flash modeling capability and was delivered for implementation in joint survivability analysis models.

15. SUBJECT TERMS
 Survivability, Operations Research, Empirical Modeling, Statistics

16. SECURITY CLASSIFICATION OF:			17. LIMITATION OF ABSTRACT	18. NUMBER OF PAGES	19a. NAME OF RESPONSIBLE PERSON
a. REPORT	b. ABSTRACT	c. THIS PAGE			Raymond R. Hill, PhD. (ENS)
U	U	U	UU	68	19b. TELEPHONE NUMBER *(Include area code)* (937) 255-3636, ext 7469; e-mail: Raymond.Hill@afit.edu